Adenovirus vector–induced IKK2^{DN} and MKK7^{DN} expression in RAW264.7 cells

A series of recent works have indicated that RANKL stimulation of osteoclast precursors activates both NF-κB and JNK pathways and that these two pathways play essential roles in the differentiation of osteoclast precursors into mature osteoclasts.[7,43,44] However, the detailed signaling events leading to their activation in osteoclast precursors still remain elusive, and the molecular interaction between these two signaling pathways is not fully understood. Previous studies show the critical implication of IKK complexes, in which IKK1 and IKK2 serve as the catalytic subunits, in NF-κB activation, and MKK4 and/or MKK7 serve as the catalytic subunits in JNK activation. To examine the role of these two signaling pathways in osteoclast development individually, we constructed adenovirus vectors carrying dominant negative IKK2 (AxIKK2^{DN}) or dominant negative MKK7 (AxMKK7^{DN}). First, to determine the efficiency of these vectors, RAW cells were infected with either AxIKK2^{DN} or AxMKK7^{DN} at different MOIs, and the expression of the proteins was examined by Western blotting with specific antibodies. It was reported that RAW cells express high levels of RANK and require RANKL but not M-CSF for their differentiation into osteoclast-like multinucleated cells.[45] As shown in Figs. 2A and 2B, both AxIKK^{DN} and AxMKK7^{DN} induced the expression of these molecules in RAW cells. No obvious morphological changes of the cells were observed even at MOI 100, and cell viability was comparable with that of AxLacZ virus–infected cells as determined by 3-(4,5-dimethylthiazol-2yl)-2,5-diphenyltetrazolium bromide (MTT) assay (Fig. 3).

Specific inhibition of NF-κB activation in RAW cells by adenovirus vector–mediated IKK2DN expression

We then examined whether overexpression of IKK2^{DN} could specifically suppress NF-κB activation by RANKL. RAW cells infected with AxIKK2^{DN} were treated with RANKL, and NF-κB activation was determined by IκB-α degradation. As shown in Fig. 4A, RANKL treatment clearly induced rapid IκB-α degradation in RAW cells, and adenovirus-mediated overexpression of IKK2^{DN} clearly inhibited the process. This also was confirmed by electrophoretic mobility shift assay (EMSA) and luciferase reporter gene assay of NF-κB as shown in Figs. 4D–4F. Importantly, RANKL-induced JNK activation was unaffected by IKK2^{DN} virus infection even at the concentration that strongly blocks NF-κB activation (Figs. 4B and 4C). These results indicate the important role of IKK2 in RANKL-induced NF-κB activation in RAW cells.

Specific inhibition of JNK activation in RAW264.7 cells by adenovirus vector–mediated MKK7^{DN} expression

In an attempt to determine if MKK7^{DN} overexpression specifically inhibits RANKL-induced JNK activation in RAW cells, AxMKK7^{DN}-infected RAW cells were stimulated with RANKL, and JNK activity was determined by Western blotting with anti–phospho-JNK antibody and by in vitro kinase assay. As shown in Figs. 5A, 5B, 5D, and 5E, RANKL-induced JNK activation was inhibited by MKK7^{DN} overexpression, and no obvious difference in NF-κB activation was observed as determined by IκB-α degradation (Fig. 5C), EMSA (Figs. 4D and 4E), and luciferase assay (Fig. 4F). MKK7^{DN} overexpression also did not affect the p38 activation in response to RANKL (data not shown). These results suggest that RANKL-induced JNK activation can be suppressed specifically by MKK7^{DN} overexpression without affecting NF-κB or p38 activation.

Overexpression of IKK2^{DN} or MKK7^{DN} inhibits osteoclast differentiation of progenitor cells

Finally, we examined the effect of these adenovirus vectors on RANKL-induced osteoclastogenesis of RAW cells. Because adenovirus infection decreased the number of adherent cells as mentioned previously, the effect of AxIKK2^{DN} or AxMKK7^{DN} on osteoclast differentiation was expressed as the proportion of TRAP$^+$ cells in the total cells. The proportion of TRAP$^+$ cells induced by RANKL was not changed by AxLacZ virus infection (data not included). To examine the importance of NF-κB activation and JNK activation in osteoclastogenesis separately, RAW cells were infected with either AxIKK2^{DN} or AxMKK7^{DN} and stimulated by sRANKL. As shown in Fig. 6, the ratio of TRAP$^+$ cells to total cells was decreased in both the AxIKK2^{DN}-infected group and the AxMKK7^{DN}-infected group in an MOI-dependent manner. These results show that both NF-κB activation and JNK activation are indispensable for RANKL-induced osteoclast differentiation.

DISCUSSION

Remarkable progress in the field of osteoclast research has been made during the last several years, especially after the discovery of OPG, RANKL, and RANK.[2] The impor-

to JNK (lower panel). (C) Fold induction of p-JNK normalized by JNK is shown. (D) The effect of overexpression of IKK2^{DN} on NF-κB activation induced by RANKL was analyzed by EMSA. RAW cells were infected with AxLacZ, AxIKK2^{DN}, or AxMKK7^{DN} and stimulated with 100 ng/ml of sRANKL as indicated. The closed and open arrowhead indicates the band of NF-κB and Rel-A supershift, respectively. The result was the representative of the experiment performed twice. (E) Fold induction of NF-κB measured by densitometry is displayed. (F) Inhibitory effect of IKK2^{DN} on NF-κB activation was confirmed also by luciferase reporter gene assay. RAW cells stably transfected with the NF-κB–dependent luciferase reporter construct were infected with AxLacZ, AxIKK2^{DN}, or AxMKK7^{DN} at the indicated MOIs. After 48 h of infection, cells were stimulated with 25 ng/ml of sRANKL and luciferase activity was measured. The relative value of the luciferase activity was plotted. Significant difference $*p < 0.001$. The significant differences were determined by analysis of variance (ANOVA) with repeated measures. Error bars represent the SD ($n = 6$).

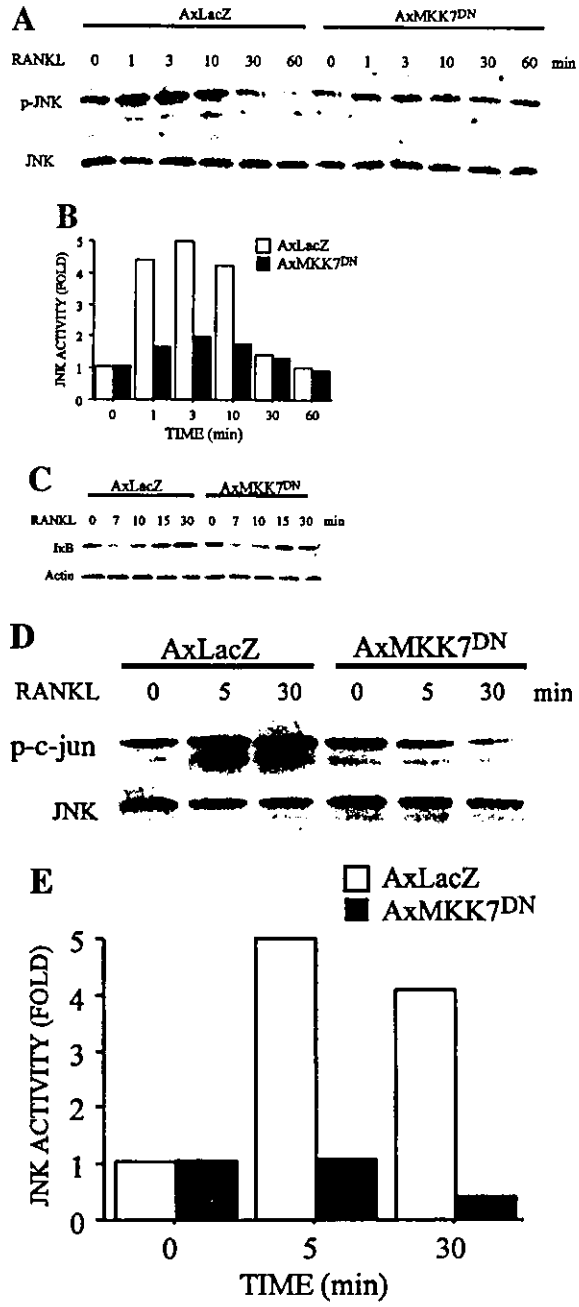

FIG. 5. Specific inhibition of RANKL-induced JNK activation in RAW cells by overexpression of MKK7^{DN}. The 10^6 RAW cells were plated on a 6-cm culture plate and infected with AxLacZ or AxMKK7^{DN} at MOI 100. Cells were further cultured for 48 h and then stimulated with 100 ng/ml sRANKL for the indicated times. (A) JNK activity was analyzed by Western blotting using antibody specific for p-JNK. The blot was stripped and reprobed with antibody specific for JNK (lower panel). (B) Fold induction of p-JNK normalized by JNK is shown. (C) Degradation of IκB-α was detected by Western blotting using specific antibody to IκB-α. The blot was stripped and reprobed with antibody specific for β-actin (lower panel). Rapid induction of IκB-α degradation was seen in both AxLacZ- and AxMKK7^{DN}-infected cells. (D) In vitro kinase assay of JNK was performed as described in the Materials and Methods section. The blot of p-c-*jun* was stripped and reprobed using specific antibody to JNK (lower panel). Inhibition of JNK activation mediated by AxMKK7^{DN} was clearly seen. (E) Fold induction of JNK is shown.

tance of the RANKL-RANK pathway in osteoclast differentiation and activation has been established by the results of the targeted disruption and overexpression of various genes involving in this signaling. Mice deficient in RANKL showed osteopetrotic pathology caused by the lack of osteoclast differentiation[7] and targeted disruption of RANK, the receptor of RANKL, also induced osteopetrosis in mice.[8,43] In contrast, a deficiency of OPG, a specific inhibitor of RANKL, caused osteoporotic skeletal changes in mice, and its overexpression led to osteopetrosis.[10,12,13] These results clearly show that the RANKL-RANK pathway plays a crucial role in osteoclast differentiation. RANK is a member of TNFR superfamily and transduces its signal through several TRAFs, including TRAF2, TRAF5, and TRAF6, followed by activation of NF-κB and JNK.[14,16–18,45,46] NF-κB is a dimerized transcription factor composed of various combinations of the structurally related proteins p50 (78 FKβ1), p52 (NFKB2), p65 (RelA), c-Rel, and RelB. NF-κB signaling pathways are involved in a wide variety of external stimuli including cytokines, pathogens, and stresses and induce a large number of genes important for cell growth, differentiation, and development. These stimuli induce phosphorylation and subsequent ubiquitination and degradation of IκB inhibitory proteins, thereby releasing NF-κB for translocation to the nucleus to function as transcription factors.[25–29] A large multiprotein complex, the IκB kinase (IKK) signalsome, was found to contain the cytokine-inducible IKK activity that phosphorylates IκB-α and IκB-β. The functional IKK complex contains IKK1 (IKKα), IKK2 (IKKβ), and NEMO (IKKγ), and IKK1 and IKK2 appear to make an important contribution to IκB phosphorylation. In spite of the high sequence similarity between IKK1 and IKK2, there exists a critical difference in their contribution to IκB phosphorylation and NF-κB activation, which was revealed by the studies of IKK1 and IKK2 knockout mice.[30–33] Stimulation of IKK1$-/-$ cells with proinflammatory cytokines resulted in normal IKK activation and IκB degradation, although NF-κB DNA-binding activity was reduced partially, indicating that IKK1 is at least partly dispensable for NF-κB activation by proinflammatory cytokines. IKK2 deficiency, in contrast, almost completely abrogates TNF-α– and interleukin (IL)-1–induced NF-κB activation. These results suggest that IKK2 is more potent for NF-κB activation by proinflammatory stimuli than IKK1. In this study, we used an adenovirus vector carrying the dominant negative mutant of IKK2 (AxIKK2^{DN}) and found that IKK2^{DN} expression remarkably suppressed the RANKL-induced NF-κB activation in RAW cells, suggesting that IKK2 plays an essential role in RANKL-induced NF-κB activation as well. JNK is activated by the phosphorylation of Thr and Tyr residues via MKK4 and/or MKK7. Previous studies showed that MKK4 is activated primarily by environmental stress and MKK7 is

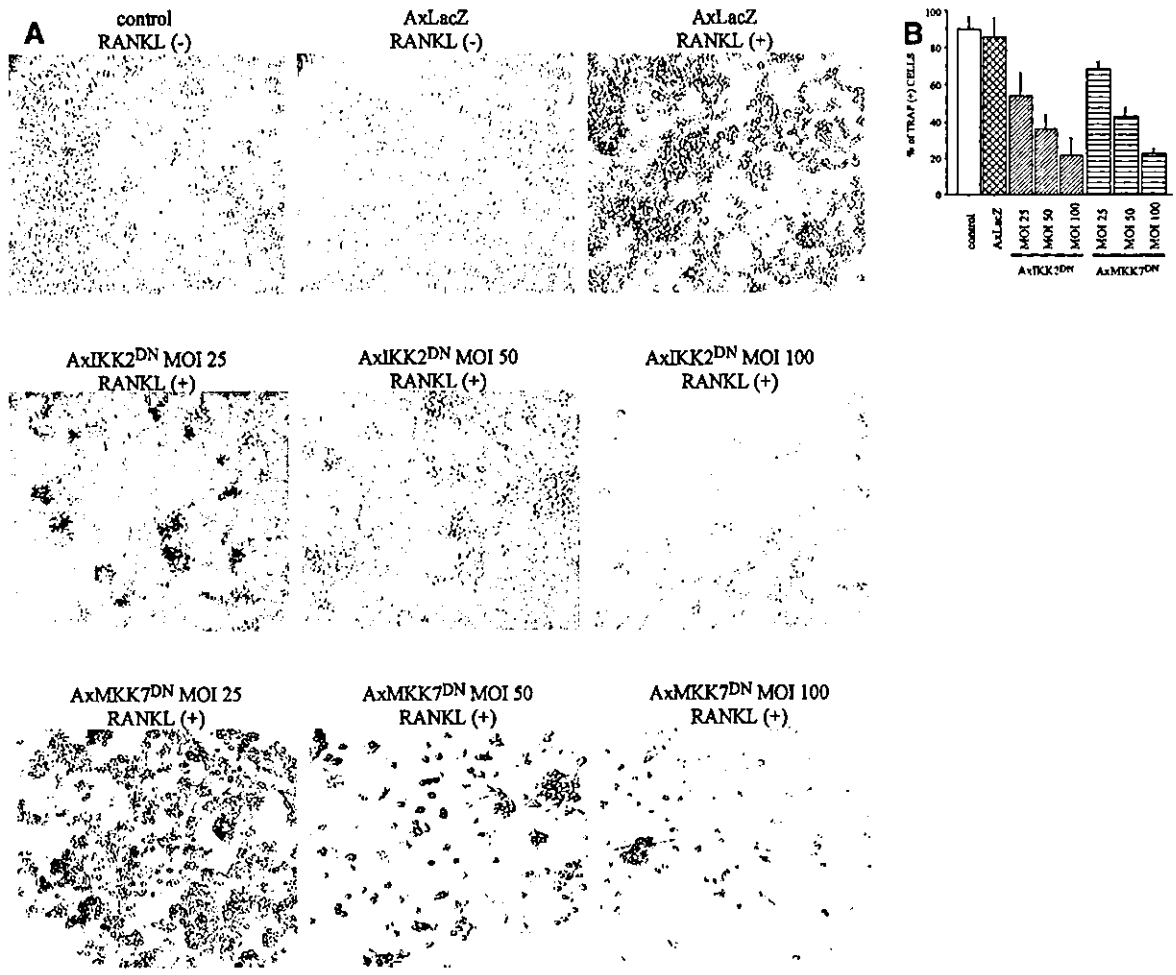

FIG. 6. Inhibition of RANKL-induced osteoclastogenesis of RAW cells by overexpression of $IKK2^{DN}$ or $MKK7^{DN}$. (A) RAW cells were infected with AxLacZ, $AxIKK2^{DN}$, or $AxMKK7^{DN}$ at the MOI indicated and stimulated with 100 ng/ml of sRANKL followed by TRAP staining. (B) The ratio of $TRAP^+$ cells to total cells was plotted. Error bars represent the SD ($n = 6$).

activated by proinflammatory cytokines.[47] To specifically inhibit JNK activation in RAW cells, we used dominant negative MKK7 because MKK4 is known to activate p38 MAPK as well and, therefore, it is possible that the dominant negative mutant of MKK4 may affect the p38 activation in response to RANKL. Overexpression of $MKK7^{DN}$ suppressed RANKL-induced JNK activation in RAW cells as shown in Figs. 5A, 5B, 5D, and 5E. This may suggest that MKK7 is the major activator of JNK in osteoclast precursors in response to RANKL, but it also is possible that MKK4 and MKK7 work together to activate JNK. Inhibition of either NF-κB or JNK activation reduced osteoclast-like cell formation in response to RANKL, indicating indispensable roles for both of these pathways in osteoclast differentiation. These results are consistent with the finding that mice deficient in both the p50 and the p52 subunits of NF-κB fail to generate mature osteoclasts and exhibit severe osteopetrosis.[19,20] JNK-induced phosphorylation of c-Jun at Ser-63 and Ser-73 increases transcriptional activity of AP-1, which is composed of various combinations of Fos and Jun family members. Because targeted disruption of c-*fos* gene also induced osteoclast deficiency in mice,[21,22] it is tempting to consider that RANKL-induced JNK activation is important for the AP-1 activation in osteoclast precursors. However, the situation seems more complicated because mutational removal of the JNK phosphorylation sites in c-Jun did not cause obvious skeletal abnormality in mice,[48] and neither JNK1 nor JNK2 knockout mice showed any skeletal abnormalities, and lack of both JNK1 and JNK2 results in embryonic lethality around E11.[49] This may suggest that JNK has an as yet undetermined role in osteoclast development other than AP-1 activation, and further investigation is required to understand precisely what the role is. Our results do not rule out the possibility that pathways other than NF-κB and JNK are required for osteoclast differentiation. In fact, overexpression of both active IKK2 and active MKK7 was not enough to induce osteoclast differentiation of RAW cells (Yamamoto et al.,

unpublished observation). Possible candidates of such pathways are the p38 MAPK and the Smad signaling. Recently, Matsumoto et al.[35] reported that RANKL activates p38 pathways in osteoclast precursors, which is essential for osteoclast differentiation, and Fuller et al.[50] and Kaneda et al.[51] showed the critical role of transforming growth factor (TGF) β in osteoclast differentiation and survival. The role of these pathways in osteoclast development should be clarified in the future. We showed efficient adenovirus vector-mediated gene transduction to RAW cells, and this system is useful for studying osteoclast differentiation. However, adenovirus infection was much less efficient in transducing primary bone marrow precursor cells (M-BMMϕ). Matsuo et al. reported an efficient gene transfer into osteoclast precursors using a retrovirus vector system.[24] However, the level of gene expression by retrovirus vectors is not enough for experiments using dominant negative molecules like this study. Developing more efficient gene transduction systems to primary osteoclast precursors will be helpful for the further analysis of the signaling pathways of osteoclast development.

ACKNOWLEDGMENT

We thank R. Yamaguchi (Department of Orthopedic Surgery, The University of Tokyo) for providing expert technical assistance and I. Verma for gifts of the AxIKK2^{DN} adenovirus. This work was supported in part by a grant-in-aid from the Ministry of Education, Science, Sports, and Culture of Japan and by the Health Science Research grants from the Ministry of Health and Welfare. S.T. received a grant from Japan Orthopaedic and Traumatology Foundation, Inc. (0113), H.O. received a Bristol-Myers Squibb/Zimmer Unrestricted Research grant, and K.N. received a Health Science Research grant from the Ministry of Health and Welfare.

REFERENCES

1. Suda T, Udagawa N, Nakamura I, Miyaura C, Takahashi N 1995 Modulation of osteoclast differentiation by local factors. Bone **17**(Suppl 2):87S–91S.
2. Suda T, Takahashi N, Udagawa N, Jimi E, Gillespie MT, Martin TJ 1999 Modulation of osteoclast differentiation and function by the new members of the tumor necrosis factor receptor and ligand families. Endocr Rev **20**:345–357.
3. Lacey DL, Timms E, Tan HL, Kelley MJ, Dunstan CR, Burgess T, Elliott R, Colombero A, Elliott G, Scully S, Hsu H, Sullivan J, Hawkins N, Davy E, Capparelli C, Eli A, Qian YX, Kaufman S, Sarosi I, Shalhoub V, Senaldi G, Guo J, Delaney J, Boyle WJ 1998 Osteoprotegerin ligand is a cytokine that regulates osteoclast differentiation and activation. Cell **93**:165–176.
4. Yasuda H, Shima N, Nakagawa N, Yamaguchi K, Kinosaki M, Mochizuki S, Tomoyasu A, Yano K, Goto M, Murakami A, Tsuda E, Morinaga T, Higashio K, Udagawa N, Takahashi N, Suda T 1998 Osteoclast differentiation factor is a ligand for osteoprotegerin/osteoclastogenesis-inhibitory factor and is identical to TRANCE/RANKL. Proc Natl Acad Sci USA **95**:3597–602.
5. Yasuda H, Shima N, Nakagawa N, Yamaguchi K, Kinosaki M, Goto M, Mochizuki SI, Tsuda E, Morinaga T, Udagawa N, Takahashi N, Suda T, Higashio K 1999 A novel molecular mechanism modulating osteoclast differentiation and function. Bone **25**:109–113.
6. Kong YY, Boyle WJ, Penninger JM 1999 Osteoprotegerin ligand: A common link between osteoclastogenesis, lymph node formation and lymphocyte development. Immunol Cell Biol **77**:188–193.
7. Kong YY, Yoshida H, Sarosi I, Tan HL, Timms E, Capparelli C, Morony S, Oliveira-dos-Santos AJ, Van G, Itie A, Khoo W, Wakeham A, Dunstan CR, Lacey DL, Mak TW, Boyle WJ, Penninger JM 1999 OPGL is a key regulator of osteoclastogenesis, lymphocyte development and lymph-node organogenesis. Nature **397**:315–323.
8. Li J, Sarosi I, Yan XQ, Morony S, Capparelli C, Tan HL, McCabe S, Elliott R, Scully S, Van G, Kaufman S, Juan SC, Sun Y, Tarpley J, Martin L, Christensen K, McCabe J, Kostenuik P, Hsu H, Fletcher F, Dunstan CR, Lacey DL, Boyle WJ 2000 RANK is the intrinsic hematopoietic cell surface receptor that controls osteoclastogenesis and regulation of bone mass and calcium metabolism. Proc Natl Acad Sci USA **97**:1566–1571.
9. Tsuda E, Goto M, Mochizuki S, Yano K, Kobayashi F, Morinaga T, Higashio K 1997 Isolation of a novel cytokine from human fibroblasts that specifically inhibits osteoclastogenesis. Biochem Biophys Res Commun **234**:137–142.
10. Simonet WS, Lacey DL, Dunstan CR, Kelley M, Chang MS, Luthy R, Nguyen HQ, Wooden S, Bennett L, Boone T, Shimamoto G, DeRose M, Elliott R, Colombero A, Tan HL, Trail G, Sullivan J, Davy E, Bucay N, Renshaw-Gegg L, Hughes TM, Hill D, Pattison W, Campbell P, Boyle WJ 1997 Osteoprotegerin: A novel secreted protein involved in the regulation of bone density. Cell **89**:309–319.
11. Mizuno A, Amizuka N, Irie K, Murakami A, Fujise N, Kanno T, Sato Y, Nakagawa N, Yasuda H, Mochizuki S, Gomibuchi T, Yano K, Shima N, Washida N, Tsuda E, Morinaga T, Higashio K, Ozawa H 1998 Severe osteoporosis in mice lacking osteoclastogenesis inhibitory factor/osteoprotegerin. Biochem Biophys Res Commun **247**:610–615.
12. Bucay N, Sarosi I, Dunstan CR, Morony S, Tarpley J, Capparelli C, Scully S, Tan HL, Xu W, Lacey DL, Boyle WJ, Simonet WS 1998 osteoprotegerin-deficient mice develop early onset osteoporosis and arterial calcification. Genes Dev **12**:1260–1268.
13. Nakagawa N, Kinosaki M, Yamaguchi K, Shima N, Yasuda H, Yano K, Morinaga T, Higashio K 1998 RANK is the essential signaling receptor for osteoclast differentiation factor in osteoclastogenesis. Biochem Biophys Res Commun **253**:395–400.
14. Darnay BG, Haridas V, Ni J, Moore PA, Aggarwal BB 1998 Characterization of the intracellular domain of receptor activator of NF-kappaB (RANK). Interaction with tumor necrosis factor receptor-associated factors and activation of NF-kappab and c-Jun N-terminal kinase. J Biol Chem **273**:20551–20555.
15. Darnay BG, Ni J, Moore PA, Aggarwal BB 1999 Activation of NF-kappaB by RANK requires tumor necrosis factor receptor-associated factor (TRAF) 6 and NF-kappaB-inducing kinase. Identification of a novel TRAF6 interaction motif. J Biol Chem **274**:7724–7731.
16. Galibert L, Tometsko ME, Anderson DM, Cosman D, Dougall WC 1998 The involvement of multiple tumor necrosis factor receptor (TNFR)-associated factors in the signaling mechanisms of receptor activator of NF-kappaB, a member of the TNFR superfamily. J Biol Chem **273**:34120–34127.
17. Lomaga MA, Yeh WC, Sarosi I, Duncan GS, Furlonger C, Ho A, Morony S, Capparelli C, Van G, Kaufman S, van der Heiden A, Itie A, Wakeham A, Khoo W, Sasaki T, Cao Z, Penninger JM, Paige CJ, Lacey DL, Dunstan CR, Boyle WJ, Goeddel DV, Mak TW 1999 TRAF6 deficiency results in osteopetrosis and defective interleukin-1, CD40, and LPS signaling. Genes Dev **13**:1015–1024.
18. Naito A, Azuma S, Tanaka S, Miyazaki T, Takaki S, Takatsu K, Nakao K, Nakamura K, Katsuki M, Yamamoto T, Inoue J 1999 Severe osteopetrosis, defective interleukin-1 signalling and lymph node organogenesis in TRAF6-deficient mice. Genes Cells **4**:353–362.

19. Iotsova V, Caamano J, Loy J, Yang Y, Lewin A, Bravo R 1997 Osteopetrosis in mice lacking NF-kappaB1 and NF-kappaB2. Nat Med **3**:1285–1289.
20. Franzoso G, Carlson L, Xing L, Poljak L, Shores EW, Brown KD, Leonardi A, Tran T, Boyce BF, Siebenlist U 1997 Requirement for NF-kappaB in osteoclast and B-cell development. Genes Dev **11**:3482–3496.
21. Wang ZQ, Ovitt C, Grigoriadis AE, Mohle-Steinlein U, Ruther U, Wagner EF 1992 Bone and haematopoietic defects in mice lacking c-*fos*. Nature **360**:741–745.
22. Johnson RS, Spiegelman BM, Papaioannou V 1992 Pleiotropic effects of a null mutation in the c-fos proto-oncogene. Cell **71**:577–586.
23. Grigoriadis AE, Wang ZQ, Cecchini MG, Hofstetter W, Felix R, Fleisch HA, Wagner EF 1994 c-Fos: A key regulator of osteoclast-macrophage lineage determination and bone remodeling. Science **266**:443–448.
24. Matsuo K, Owens JM, Tonko M, Elliott C, Chambers TJ, Wagner EF 2000 Fosl1 is a transcriptional target of c-Fos during osteoclast differentiation. Nat Genet **24**:184–187.
25. Verma IM, Stevenson JK, Schwarz EM, Van Antwerp D, Miyamoto S 1995 Rel/NF-kappa B/I kappa B family: Intimate tales of association and dissociation. Genes Dev **9**:2723–2735.
26. Verma IM, Stevenson J 1997 IkappaB kinase: Beginning, not the end. Proc Natl Acad Sci USA **94**:11758–11760.
27. Karin M 1999 The beginning of the end: IkappaB kinase (IKK) and NF-kappaB activation. J Biol Chem **274**:27339–27342.
28. Ghosh S, May MJ, Kopp EB 1998 NF-kappa B and Rel proteins: Evolutionarily conserved mediators of immune responses. Annu Rev Immunol **16**:225–260.
29. Ghosh S 1999 Regulation of inducible gene expression by the transcription factor NF-kappaB. Immunol Res **19**:183–189.
30. Li Q, Van Antwerp D, Mercurio F, Lee KF, Verma IM 1999 Severe liver degeneration in mice lacking the IkappaB kinase 2 gene. Science **284**:321–325.
31. Li Q, Lu Q, Hwang JY, Buscher D, Lee KF, Izpisua-Belmonte JC, Verma IM 1999 IKK1-deficient mice exhibit abnormal development of skin and skeleton. Genes Dev **13**:1322–1328.
32. Li ZW, Chu W, Hu Y, Delhase M, Deerinck T, Ellisman M, Johnson R, Karin M 1999 The IKKbeta subunit of IkappaB kinase (IKK) is essential for nuclear factor kappaB activation and prevention of apoptosis. J Exp Med **189**:1839–1845.
33. Rudolph D, Yeh WC, Wakeham A, Rudolph B, Nallainathan D, Potter J, Elia AJ, Mak TW 2000 Severe liver degeneration and lack of NF-kappaB activation in NEMO/IKKgamma-deficient mice. Genes Dev **14**:854–862.
34. Kobayashi K, Takahashi N, Jimi E, Udagawa N, Takami M, Kotake S, Nakagawa N, Kinosaki M, Yamaguchi K, Shima N, Yasuda H, Morinaga T, Higashio K, Martin TJ, Suda T 2000 Tumor necrosis factor alpha stimulates osteoclast differentiation by a mechanism independent of the ODF/RANKL-RANK interaction. J Exp Med **191**:275–286.
35. Matsumoto M, Sudo T, Saito T, Osada H, Tsujimoto M 2000 Involvement of p38 mitogen-activated protein kinase signaling pathway in osteoclastogenesis mediated by receptor activator of NF-kappa B ligand (RANKL). J Biol Chem **275**:31155–31161.
36. He TC, Zhou S, da Costa LT, Yu J, Kinzler KW, Vogelstein B 1998 A simplified system for generating recombinant adenoviruses. Proc Natl Acad Sci USA **95**:2509–2514.
37. Kanegae Y, Makimura M, Saito I 1994 A simple and efficient method for purification of infectious recombinant adenovirus. Jpn J Med Sci Biol **47**:157–166.
38. Tanaka S, Takahashi T, Takayanagi H, Miyazaki T, Oda H, Nakamura K, Hirai H, Kurokawa T 1998 Modulation of osteoclast function by adenovirus vector-induced epidermal growth factor receptor. J Bone Miner Res **13**:1714–1720.
39. Matsuyama T, Kimura T, Kitagawa M, Pfeffer K, Kawakami T, Watanabe N, Kundig TM, Amakawa R, Kishihara K, Wakeham A 1993 Targeted disruption of IRF-1 or IRF-2 results in abnormal type I IFN gene induction and aberrant lymphocyte development. Cell **75**:83–97.
40. Takayanagi H, Juji T, Miyazaki T, Iizuka H, Takahashi T, Isshiki M, Okada M, Tanaka Y, Koshihara Y, Oda H, Kurokawa T, Nakamura K, Tanaka S 1999 Suppression of arthritic bone destruction by adenovirus-mediated csk gene transfer to synoviocytes and osteoclasts. J Clin Invest **104**:137–146.
41. Miyazaki T, Takayanagi H, Isshiki M, Takahashi T, Okada M, Fukui Y, Oda H, Nakamura K, Hirai H, Kurokawa T, Tanaka S 2000 In vitro and in vivo suppression of osteoclast function by adenovirus vector-induced csk gene. J Bone Miner Res **15**:41–51.
42. Miyazaki T, Katagiri H, Kanegae Y, Takayanagi H, Sawada Y, Yamamoto A, Pando MP, Asano T, Verma IM, Oda H, Nakamura K, Tanaka S 2000 Reciprocal role of ERK and NF-kappaB pathways in survival and activation of osteoclasts. J Cell Biol **148**:333–342.
43. Dougall WC, Glaccum M, Charrier K, Rohrbach K, Brasel K, De Smedt T, Daro E, Smith J, Tometsko ME, Maliszewski CR, Armstrong A, Shen V, Bain S, Cosman D, Anderson D, Morrissey PJ, Peschon JJ, Schuh J 1999 RANK is essential for osteoclast and lymph node development. Genes Dev **13**:2412–2424.
44. Jimi E, Akiyama S, Tsurukai T, Okahashi N, Kobayashi K, Udagawa N, Nishihara T, Takahashi N, Suda T 1999 Osteoclast differentiation factor acts as a multifunctional regulator in murine osteoclast differentiation and function. J Immunol **163**:434–442.
45. Hsu H, Lacey DL, Dunstan CR, Solovyev I, Colombero A, Timms E, Tan HL, Elliott G, Kelley MJ, Sarosi I, Wang L, Xia XZ, Elliott R, Chiu L, Black T, Scully S, Capparelli C, Morony S, Shimamoto G, Bass MB, Boyle WJ 1999 Tumor necrosis factor receptor family member RANK mediates osteoclast differentiation and activation induced by osteoprotegerin ligand. Proc Natl Acad Sci USA **96**:3540–3545.
46. Wong BR, Josien R, Lee SY, Vologodskaia M, Steinman RM, Choi Y 1998 The TRAF family of signal transducers mediates NF-kappaB activation by the TRANCE receptor. J Biol Chem **273**:28355–28359.
47. Roger JD 2000 Signal transduction by the JNK group of MAP kinases. Cell **103**:239–252.
48. Behrens A, Sibilia M, Wagner EF 1999 Amino-terminal phosphorylation of c-Jun regulates stress-induced apoptosis and cellular proliferation. Nat Genet **21**:326–329.
49. Sabapathy K, Jochum W, Hochedlinger K, Chang L, Karin M, Wagner EF 1999 Defective neural tube morphogenesis and altered apoptosis in the absence of both JNK1 and JNK2. Mech Dev **89**:115–124.
50. Fuller K, Lean JM, Bayley KE, Wani MR, Chambers TJ 2000 A role for TGFbeta(1) in osteoclast differentiation and survival. J Cell Sci **113**:2445–2453.
51. Kaneda T, Nojima T, Nakagawa M, Ogasawara A, Kaneko H, Sato T, Mano H, Kumegawa M, Hakeda Y 2000 Endogenous production of TGF-beta is essential for osteoclastogenesis induced by a combination of receptor activator of NF-kappaB ligand and macrophage-colony- stimulating factor. J Immunol **165**:4254–4263.

Address reprint requests to:
Sakae Tanaka, M.D., Ph.D.
Department of Orthopedic Surgery
Faculty of Medicine
The University of Tokyo
7–3–1 Hongo, Bunkyo-ku
Tokyo 113-0033, Japan

Received in original form April 3, 2001; in revised form August 9, 2001; accepted September 5, 2001.

IL-1 Regulates Cytoskeletal Organization in Osteoclasts Via TNF Receptor-Associated Factor 6/c-Src Complex[1]

Ichiro Nakamura,[2*†] Yuho Kadono,[*] Hiroshi Takayanagi,[*] Eijiro Jimi,[‡] Tsuyoshi Miyazaki,[*] Hiromi Oda,[*] Kozo Nakamura,[*] Sakae Tanaka,[*] Gideon A. Rodan,[†] and Le T. Duong[†]

Targeted disruption of either c-Src or TNFR-associated factor 6 (TRAF6) in mice causes osteoclast dysfunction and an osteopetrotic phenotype, suggesting that both molecules play important roles in osteoclastic bone resorption. We previously demonstrated that IL-1 induces actin ring formation and osteoclast activation. In this study, we examined the relationship between IL-1/TRAF6-dependent and c-Src-mediated pathways in the activation of osteoclast-like cells (prefusion cells (pOCs); multinucleated cells) formed in the murine coculture system. In normal pOCs, IL-1 induces actin ring formation and tyrosine phosphorylation of $p130^{Cas}$, a known substrate of c-Src. However, in Src-deficient pOCs, $p130^{Cas}$ was not tyrosine phosphorylated following IL-1 treatment. In normal pOCs treated with IL-1, anti-TRAF6 Abs coprecipitate $p130^{Cas}$, protein tyrosine kinase 2, and c-Src. In Src-deficient pOCs, this molecular complex was not detected, suggesting that c-Src is required for formation of the TRAF6, $p130^{Cas}$, and protein tyrosine kinase 2 complex. Moreover, an immunocytochemical analysis revealed that in osteoclast-like multinucleated cells, IL-1 induced redistribution of TRAF6 to actin ring structures formed at the cell periphery, where TRAF6 also colocalized with c-Src. Taken together, these data suggest that IL-1 signals feed into the tyrosine kinase pathways through a TRAF6-Src molecular complex, which regulates the cytoskeletal reorganization essential for osteoclast activation. *The Journal of Immunology,* 2002, 168: 5103–5109.

Interleukin-1 is a multifunctional cytokine that regulates various cellular and tissue functions (1). Bone is one of the most sensitive tissues to IL-1 (2–4). IL-1 exhibits potent bone-resorbing activity in vivo (3) and in vitro (2, 4), and the natural inhibitory protein, IL-1R antagonist, blocks the ability of IL-1 to stimulate bone resorption in organ culture (5) and in ovariectomized rats in vivo (6). Several lines of evidence suggest that IL-1 is also involved in the bone destruction associated with multiple myeloma, rheumatoid arthritis, and osteoporosis (1).

Osteoclasts, the bone-resorbing cells, are macrophage-related multinucleated cells that play a critical role in bone remodeling (7, 8). Osteoclastic bone resorption consists of multiple steps: proliferation of osteoclast progenitors, differentiation of progenitors into mononuclear prefusion osteoclasts (pOCs),[3] fusion of pOCs into osteoclast-like multinucleated cells (OCLs), sealing zone (actin ring) and ruffled border formation, the active resorption, and eventually apoptosis. In vitro evidence indicates that IL-1 participates in the following steps: 1) IL-1 stimulates osteoclast formation indirectly by stimulating PGE_2 synthesis in osteoblasts/stromal cells (9); 2) IL-1 induces fusion of mononuclear osteoclasts, leading to multinucleation (10); 3) IL-1 potentiates osteoclast function (pit-forming activity) directly (10) or indirectly via osteoblasts (11); 4) and finally, IL-1 is directly involved in prolonging osteoclast life span (12–14).

The objective of this study was to investigate the intracellular signaling involved in osteoclast activation by IL-1. After IL-1 binding, the IL-1R-associated kinase (IRAK), a serine/threonine kinase, becomes autophosphorylated and is recruited to the receptor complex by binding to MyD88. Another adapter, TNFR-associated factor 6 (TRAF6), then interacts with IRAK (15). Interestingly, targeted disruption of TRAF6 in mice results in osteoclast dysfunction and in osteopetrotic phenotype (16), which is similar to that in c-Src-deficient mice (17, 18), suggesting that both molecules play important roles in osteoclastic bone resorption. In this study, we examined the relationship between IL-1/TRAF6-dependent and c-Src-mediated pathways in osteoclast-like cells derived from the in vitro coculture system, and showed that IL-1 cross-regulates the tyrosine kinase pathway via the association of TRAF6 and c-Src, leading to osteoclast cytoskeletal rearrangement and activation.

Materials and Methods

Abs and other reagents

Vitronectin (Vn) and poly(L-lysine) (PL) were from Life Technologies (Grand Island, NY) and Sigma-Aldrich (St. Louis, MO), respectively. Abs specific to c-Src (N-16) and TRAF6 (H-274 and D-10) were from Santa Cruz Biotechnology (Santa Cruz, CA); $p130^{Cas}$ (mAb 21) and protein tyrosine kinase 2 (PYK2) (mAb 11) from BD Transduction Laboratories (Lexington, KY); phosphotyrosine (4G10) and c-Src (GD11) from Upstate Biotechnology (Lake Placid, NY); and c-Src (mAb 327) from Oncogene Research Products (Cambridge, MA). Other conjugated secondary Abs were from Jackson ImmunoResearch Laboratories (West Grove, PA) and Amersham (Arlington Heights, IL). The 1α,25-dihydroxyvitamin D3 (1α,25(OH)2D3) and collagenase were from WAKO (Dallas, TX), and dispase was from Boehringer Mannheim (Indianapolis, IN). Human rIL-1α and murine M-CSF were from R&D Systems (Minneapolis, MN).

*Department of Orthopedic Surgery, Faculty of Medicine, University of Tokyo, Tokyo, Japan; †Department of Bone Biology and Osteoporosis Research, Merck Research Laboratories, West Point, PA 19486; and ‡Section of Immunobiology, Yale University, School of Medicine, New Haven, CT 06520

Received for publication May 11, 2001. Accepted for publication March 15, 2002.

The costs of publication of this article were defrayed in part by the payment of page charges. This article must therefore be hereby marked *advertisement* in accordance with 18 U.S.C. Section 1734 solely to indicate this fact.

[1] This work was in part supported by Takeda Science Foundation (to I.N.), Health Science Research Grants from Ministry of Health and Welfare (to S.T.), and Uehara Memorial Foundation (to S.T.).

[2] Address correspondence and reprint requests to Dr. Ichiro Nakamura at the current address: Department of Orthopedic Surgery, Yugawara Kosei-nenkin Hospital, 438 Miyakami, Yugawara, Ashigara-shimo-gun, Kanagawa 259-0314, Japan. E-mail address: Ichiclast@aol.com

[3] Abbreviations used in this paper: pOC, prefusion osteoclast-like cell; 1α,25(OH)2D3, 1α,25-dihydroxyvitamin D3; Cas, Crk-associated substrate; IRAK, IL-1R-associated kinase; OCL, osteoclast-like multinucleated cell; PL, poly(L-lysine); PYK2, protein tyrosine kinase 2; RANK, receptor activator of NF-κB; SH, Src homology; TRAF6, TNFR-associated factor 6; Vn, vitronectin.

0022-1767/02/$02.00

Animals

BALB/c mice were obtained from Taconic Farms (Germantown, NY). Heterozygote $Src^{+/-}$ mice obtained from The Jackson Laboratory (Bar Harbor, ME) were mated in our laboratory, and $Src^{-/-}$ mice were phenotypically distinguished from their $Src^{+/?}$ siblings by lack of tooth eruption. All animals were cared for according to the Institutional Animal Care and Use Committee Guide.

Cell cultures

pOCs were prepared as described previously, with slight modifications (19). Briefly, spleen cells isolated from 2- to 3-wk-old $Src^{-/-}$ or their normal littermates were cocultured with osteoblastic MB1.8 cells for 5–6 days in the presence of 10 nM 1α,25(OH)2D3. pOCs were released from dishes with 10 mM EDTA after removing MB1.8 cells with collagenase-dispase.

Murine OCLs were prepared using BALB/c mice, as described previously (20). Primary osteoblastic cells were obtained from newborn mouse calvaria, and bone marrow cells were obtained from tibiae of 7- to 9-wk-old male mice. Cells were cocultured in α-MEM containing 10% FBS and 10 nM 1α,25(OH)2D3 on culture dishes precoated with 5 ml 0.2% collagen gel matrix (Nitta Gelatin, Osaka, Japan). OCLs were formed within 7 days of culture, and were released from the dishes by treatment with 5 ml 0.2% collagenase, before being collected by centrifugation at 250 × *g* for 5 min (crude OCL preparation). Crude OCL preparations were cultured on culture dishes or glass coverslips for 4 h and then purified by collagenase and dispase (purified OCL preparation).

Cell adhesion and IL-1 treatment

After isolation, pOCs (8 × 10^5cells/condition) were washed twice with serum-free α-MEM medium containing 0.1% BSA (Sigma-Aldrich) and allowed to attach to polystyrene dishes coated with Vn (20 μg/ml) or PL (50 μg/ml). After culture for 60 min, cells were treated with IL-1 (10 ng/ml) for the indicated periods, and an equal volume of 2× TNE lysis buffer (20 mM Tris (pH 7.8), 300 mM NaCl, 2 mM EDTA, 2% Nonidet P-40, 2 mM Na_3VO_4, 20 mM NaF, 20 μg/ml leupeptin, 10 μg/ml aprotinin, and 2 mM PMSF) was added to the plates. For coimmunoprecipitation, 1.5 × 10^6 cells/condition and 1× TNE lysis buffer with 10% glycerol (10 nM Tris (pH 7.8), 300 mM NaCl, 1 mM EDTA, 1% Nonidet P-40, 1 mM Na_3VO_4, 10 mM NaF, 10 μg/ml leupeptin, 0.5 TIU/ml aprotinin, 1 mM PMSF, and 10% glycerol) were used. Clarified lysates were subjected to immunoprecipitation and immunoblotting. Alternatively, cells were fixed and stained for tartrate-resistant acid phosphatase, a marker enzyme of osteoclasts, and F-actin (20).

Analysis of kinase activity of c-Src

Osteoclast-like cells were prepared as described previously, with slight modifications (21). After the removal of bone marrow stromal cells, nonadherent bone marrow cells (2.5 × 10^5/well in six-well plates) were cultured in α-MEM containing 10% FBS and 10 ng/ml M-CSF for 3 days, and adherent cells were subsequently used as bone marrow monocyte/macrophage precursor cells after washing out the nonadherent cells, including lymphocytes. The bone marrow monocyte/macrophage precursor cells were further cultured in the presence of 100 ng/ml soluble receptor activator of NF-κB (RANK) ligand (Peprotech, Rocky Hill, NJ) and 10 ng/ml M-CSF to generate murine osteoclast-like cells. After 3 days, the medium was changed to serum-free α-MEM for 2 h before stimulation with 10 ng/ml IL-1. At the indicated time points, whole cell lysates were prepared and assayed for the kinase activity using poly(Glu-Tyr) as a substrate after immunoprecipitation with anti-v-Src Ab by universal tyrosine kinase assay kit (Takara, Tokyo, Japan), according to the manufacturer's protocol. A

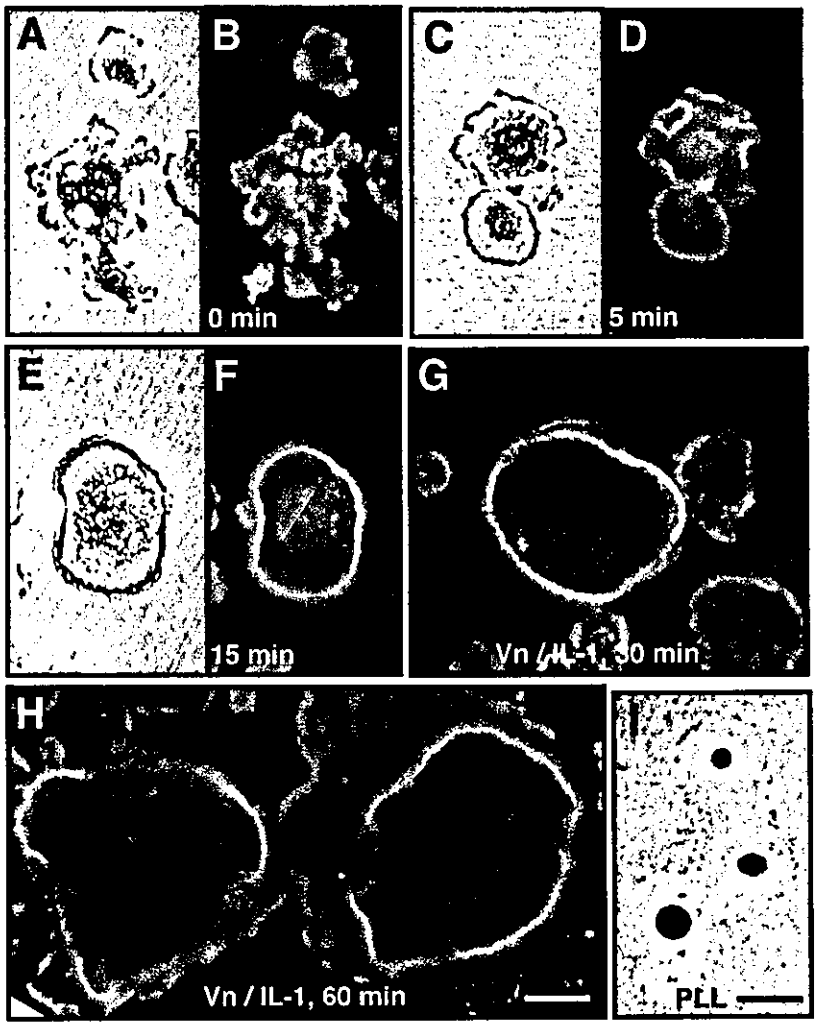

FIGURE 1. Effect of IL-1 on actin ring formation of pOCs. $Src^{+/?}$ pOCs were plated on Vn (20 μg/ml) (*A–H*)- or PL (50 μg/ml) (*I*)-coated dishes in the absence of serum. After culture for 60 min, cells were treated with IL-1 (10 ng/ml) for 0 (*A*, *B*, and *I*), 5 (*C* and *D*), 15 (*E* and *F*), 30 (*G*), and 60 (*H*) min. Cells were fixed and stained for tartrate-resistant acid phosphatase (*A*, *C*, *E* and *I*) or F-actin (*B*, *D*, *F*, *G* and *H*). Bar = 20 μm.

unit of c-Src kinase activity is defined as an activity to incorporate 1 pmol phosphate into a substrate (KVEKIGEGTYGVVYK) per minute.

Immunoblotting and immunoprecipitation

Immunoprecipitation and immunoblotting were performed as previously described (22). Briefly, lysates were precipitated with anti-p130^{Cas}, TRAF6, or c-Src Abs (2 μg) for 2 h at 4°C, followed by protein G-Sepharose for 1 h at 4°C. After washing with lysis buffer (four times), proteins were separated on an 8% SDS-PAGE and blotted onto Immobilon-P membrane (Millipore, Bedford, MA). After blocking with 100 mM NaCl, 10 mM Tris, 0.1% Tween 20, and 2% BSA, the membrane was incubated with primary Abs, followed by HRP-conjugated secondary Abs, and detected with the ECL system (Amersham).

Immunofluorescence

Crude preparations of OCLs were seeded on glass coverslips. After culture for 4 h, osteoclasts were purified as described above, serum starved for 4 h, and then treated with or without 10 ng/ml IL-1 for 30 min. Cells were fixed with 4% paraformaldehyde, permeabilized with 0.5% Triton X-100 in PBS, and incubated for 30 min at 37°C with rabbit anti-TRAF6 polyclonal (H-274) or anti-c-Src mAb 327 Abs. Cells were washed with PBS and incubated for 30 min at 37°C with Cy3-conjugated goat anti-rabbit IgG (Jackson ImmunoResearch Laboratories), FITC-conjugated goat anti-mouse IgG (Jackson ImmunoResearch Laboratories), or Oregon Green 488 phalloidin (Molecular Probes, Eugene, OR). Samples were viewed with a confocal microscope (Radiance; Bio-Rad, Hercules, CA).

Preparation of nuclear proteins

Purified OCLs treated with or without IL-1 for 30 min were washed, collected with 1 ml 0.1% BSA in PBS, and spinned down for 2 min at 3000 rpm. The pellet was resuspended in 200 μl ice-cold buffer A (10 mM HEPES (pH 7.9), 10 mM KCl, 0.1 mM EDTA, 1 mM PMSF, 1 TIU/ml aprotinin, 10 mM NaF, and 1 mM DTT) and left to swell on ice for 10 min. After the addition of 1% Nonidet P-40 detergent (10 μl), lysates were subjected to vortexing for 30 s and centrifuged for 5 min at 3000 rpm. The pellets were washed once in buffer A (100 μl), centrifuged at 1.5 min at 3000 rpm, replaced with 50 μl buffer B (20 mM HEPES (pH 7.9), 0.4 M NaCl, 1 mM EDTA, 1 mM PMSF, 10 μm/ml aprotinin, 10 mM NaF, and 1 mM DTT), and then shaken vigorously at 4°C for >15 min. Subsequently, the mixture was centrifuged for 20 min at 14,000 rpm. Finally, the supernatant was recovered and used as source for nuclear proteins. To determine the purity of the nuclear extract preparations, PYK2 was used as an abundant cytosolic marker in osteoclasts. When proteins (25 μg) isolated from nuclear and cytosolic fractions were subjected to Western blotting for PYK2, the level of PYK2 detected in nuclear extract was about 5% of that in the cytosol (data not shown), suggesting that the purity of the nuclear extracts was >90%.

Results

Effect of IL-1 on actin ring formation of pOCs

It was previously shown that IL-1 induces actin ring formation, leading to osteoclast activation (10). In this study, we confirmed these findings in a serum-free system. pOCs were prepared from the murine coculture system and plated on Vn-coated dishes in the absence of serum. pOCs spread on Vn-coated surfaces 60 min after plating (Fig. 1*A*), whereas on PL they remain rounded (Fig. 1*I*). Initial adhesion to Vn did not induce actin ring formation (Fig. 1*B*); however, after treatment with IL-1, these cells started to form actin rings in a time-dependent manner (Fig. 1*C–H*).

Effect of IL-1 on tyrosine phosphorylation of p130^{Cas} and c-Src kinase activity

We previously reported on the role of p130^{Cas} and PYK2 in the $\alpha_v\beta_3$ integrin-mediated signaling pathways that lead to actin ring formation in osteoclasts (22–25). We therefore examined the involvement of p130^{Cas} in IL-1-induced actin ring formation. Tyrosine phosphorylation of p130^{Cas} and PYK2 following cell adhesion peaks at 30–60 min after plating (22, 24, 25). pOCs were therefore plated on PL- or Vn-coated dishes for 60 min and then treated with or without IL-1 for 30 min. Cell lysates from these samples were immunoprecipitated with anti-p130^{Cas} Abs and analyzed by Western blotting with anti-phosphotyrosine Abs. As reported previously (24, 25), cell adhesion resulted in tyrosine phosphorylation of p130^{Cas} (Fig. 2*A*, *left upper panel*). Interestingly, IL-1 increased the tyrosine phosphorylation of p130^{Cas} (Fig. 2*A*, *left upper panel*), suggesting that p130^{Cas} might be a downstream mediator of the IL-1R-dependent signaling pathway. PYK2 was also tyrosine phosphorylated not only by cell adhesion to Vn, but also by IL-1 treatment (data not shown).

Several lines of evidence, including our previous findings, have shown that tyrosine phosphorylation of p130^{Cas} is mediated by Src kinase and that c-Src deficiency abrogated adhesion-induced p130^{Cas} phosphorylation in fibroblasts and osteoclasts (23–27). We examined therefore the involvement of c-Src in IL-1-induced tyrosine phosphorylation of p130^{Cas}, using Src-deficient pOCs. As shown in Fig. 2*A* (*right upper panel*), neither cell adhesion to Vn nor IL-1 treatment induced tyrosine phosphorylation of p130^{Cas}. Furthermore, nor did IL-1 induce actin ring formation and pit-forming activity in Src$^{-/-}$ pOCs (data not shown). These data suggest that c-Src may play an important role in IL-1-induced tyrosine phosphorylation of p130^{Cas} and its osteoclast activation.

To support the above notion, we also examined the effect of IL-1 on c-Src kinase activity using poly(Glu-Tyr) as a substrate. As shown in Fig. 2*B*, IL-1 induces activation of c-Src within 5 min after treatment,

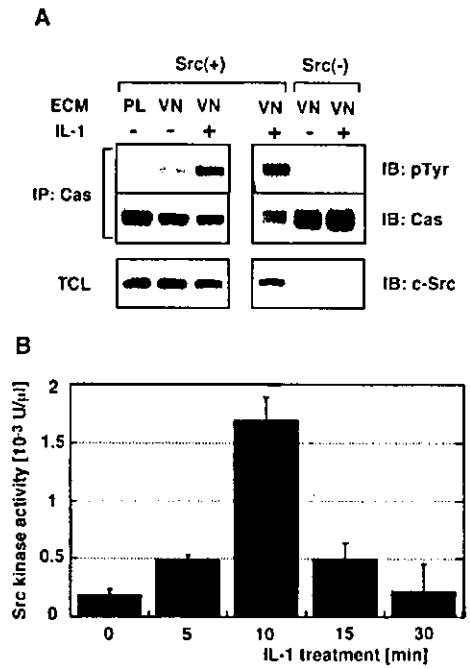

FIGURE 2. Effects of IL-1 on tyrosine phosphorylation of p130^{Cas} and c-Src kinase activity in pOCs. *A*, Src$^{+/?}$ or Src$^{-/-}$ pOCs were plated on Vn (20 μg/ml)- or PL (50 μg/ml)-coated dishes in the absence of serum. After culture for 60 min, cells were treated with or without IL-1 (10 ng/ml) for 30 min. Total cell lysates were immunoprecipitated with anti-p130^{Cas} Ab, followed by immunoblotting with anti-phosphotyrosine (pTyr) Ab (*upper panels*). The same membranes were stripped and blotted with anti-Cas Ab (*middle panels*). Total cell lysates were also subjected to immunoblotting with anti-c-Src Ab (*lower panels*). ECM, IB, IP, and TCL: extracellular matrix, total cell lysate, immunoblotting, and immunoprecipitation, respectively. *B*, Osteoclast-like cells were prepared as described in *Materials and Methods*. Cells were serum starved for 2 h before treating with 10 ng/ml IL-1. After the indicated periods, whole cell lysates were extracted and assayed for the kinase activity using poly(Glu-Tyr) as a substrate after immunoprecipitation with anti-v-Src Ab by universal tyrosine kinase assay kit. A unit of c-Src kinase activity is defined as an activity to incorporate 1 pmol phosphate into a substrate (KVEKIGEGTYGVVYK) per minute.

suggesting that c-Src activity might be directly regulated by the IL-1 signaling pathway, leading to the tyrosine phosphorylation of downstream mediators such as $p130^{Cas}$ and PYK2.

IL-1 induces association of TRAF6 and c-Src

Among members of the TRAF family adapter proteins, TRAF6 is to date the only one mediating IL-1 signaling, through its interaction with the IRAK (28). We therefore examined the relationship of TRAF6 with IL-1-induced tyrosine-phosphorylated proteins in osteoclasts. $Src^{+/?}$ pOCs were plated on PL- or Vn-coated dishes for 60 min and then treated with or without IL-1 for 30 min. Cell lysates were immunoprecipitated with anti-TRAF6 Ab and analyzed by Western blotting with anti-phosphotyrosine Ab. Interestingly, from lysates of cells plated on Vn and treated with IL-1, anti-TRAF6 Abs coprecipitated at least three tyrosine-phosphorylated proteins with molecular mass values of about 130, 120, and 60 kDa (Fig. 3*A*, *lanes 1–3*, arrowheads). Western blotting of the same membrane revealed that anti-TRAF6 Ab coprecipitated c-Src (~60 kDa), PYK2 (~110–120 kDa), and $p130^{Cas}$ (~130 kDa) (Fig. 3*A*, *lanes 4–9*), suggesting that these three proteins could be the major tyrosine-phosphorylated proteins in IL-1-treated cells. In contrast, we could not rule out additional unidentified proteins with similar molecular masses could be tyrosine phosphorylated in IL-1-treated osteoclasts. These observations indicate that IL-1 treatment induces the formation of a complex containing TRAF6, c-Src, PYK2, and $p130^{Cas}$ in osteoclasts on Vn. Adhesion appears to be a prerequisite for IL-1/TRAF6-dependent association with c-Src, PYK2, and $p130^{Cas}$, because IL-1 treatment of pOCs on PL or in suspension did not result in the same complex formation (data not shown).

We next asked which molecule is essential for the formation of this complex with TRAF6. To address this question, we plated

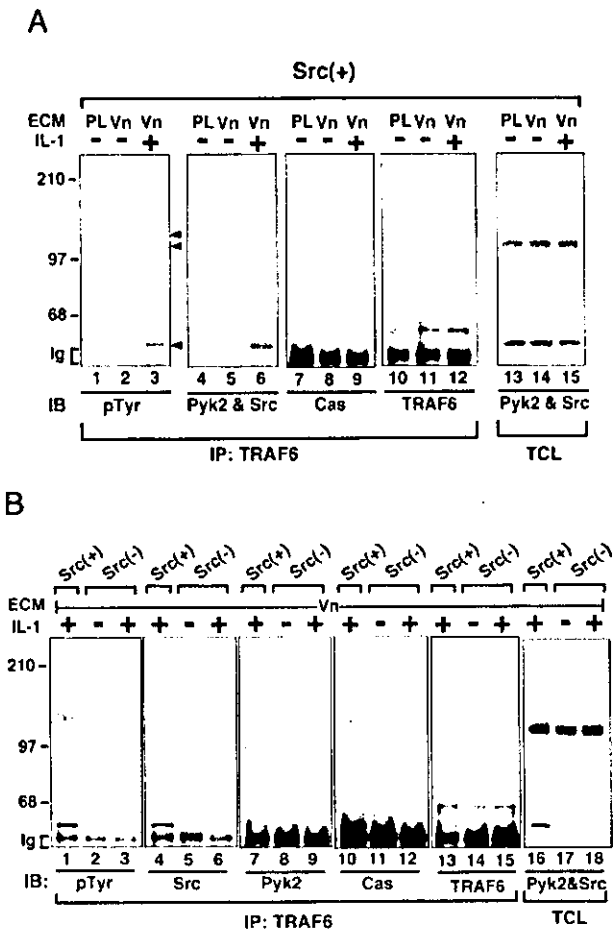

FIGURE 3. Association of TRAF6 with c-Src, PYK2, and $p130^{Cas}$ in pOCs. *A*, $Src^{+/?}$ pOCs (1.5×10^6 cells/condition) were plated on Vn (20 μg/ml)- or PL (50 μg/ml)-coated dishes in the absence of serum. After culture for 60 min, cells were treated with or without IL-1 (10 ng/ml) for 30 min. Total cell lysates (>1 mg/ml) were immunoprecipitated with anti-TRAF6 Ab (H-274) (*lanes 1–12*), followed by immunoblotting with anti-phosphotyrosine Ab (*lanes 1–3*). The same membrane was sequentially stripped and blotted with anti-PYK2 and c-Src (*lanes 4–6*), anti-$p130^{Cas}$ (*lanes 7–9*), and anti-TRAF6 (D-10) (*lanes 10–12*) Abs. Total cell lysates were also subjected to immunoblotting with anti-c-Src and PYK2 Abs (*lanes 13–15*). *B*, $Src^{+/?}$ (*lanes 1, 4, 7, 10, 13,* and *16*) and $Src^{-/-}$ (*lanes 2, 3, 5, 6, 8, 9, 11, 12, 14, 15, 17,* and *18*) pOCs were plated on Vn- or PL-coated dishes in the absence of serum. After culture for 60 min, cells were treated with or without IL-1 for 30 min. Total cell lysates (>1 mg/ml) were immunoprecipitated with anti-TRAF6 Ab (H-274) (*lanes 1–15*), followed by immunoblotting with anti-phosphotyrosine Ab (*lanes 1–3*). The same membrane was sequentially stripped and blotted with anti-c-Src (*lanes 4–6*), anti-PYK2 (*lanes 7–9*), anti- $p130^{Cas}$ (*lanes 10–12*), and anti-TRAF6 (D-10) (*lanes 13–15*) Abs. Total cell lysates were also subjected to immunoblotting with anti-c-Src and PYK2 Abs (*lanes 16–18*). The molecular masses of marker proteins are indicated in kDa on the *left*. ECM, IB, IP, TCL, and pTyr: extracellular matrix, immunoblotting, immunoprecipitation, total cell lysate, and phosphotyrosine, respectively.

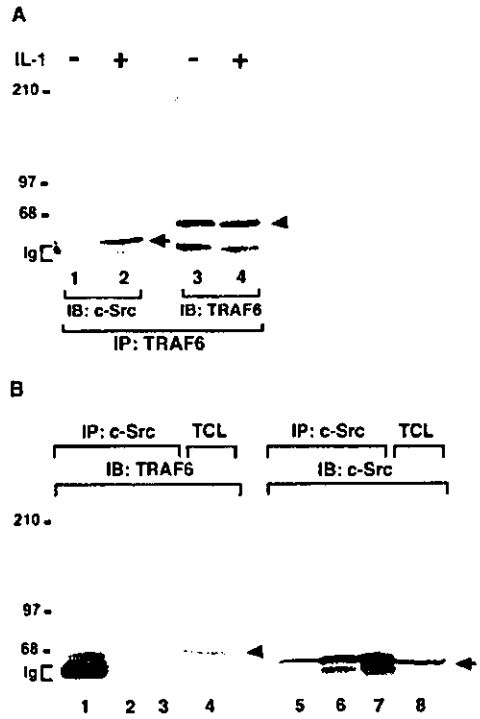

FIGURE 4. Association of TRAF6 and c-Src in OCLs. Purified OCLs were prepared as described in *Materials and Methods*. *A*, After culture for 4 h in the absence of serum, cells were treated with (*lanes 2* and *4*) or without 10 ng/ml IL-1 (*lanes 1* and *3*) for 30 min. Total cell lysates (>1 mg/ml) were immunoprecipitated with anti-TRAF6 (H-274) Ab, followed by immunoblotting with anti-c-Src (GD11). The same membrane was stripped and blotted with anti-TRAF6 Ab (D-10). *B*, Purified OCLs were treated with IL-1 (10 ng/ml) for 30 min. Total cell lysates (>1 mg/ml) were immunoprecipitated with anti-c-Src (*lane 1*, N-16; *lane 2*, mAb327; *lane 3*, GD11) Abs, followed by immunoblotting with anti-TRAF6 Ab (H-274). The same membrane was stripped and blotted with anti-c-Src Ab (GD11). The molecular masses of marker proteins are indicated in kDa on the *left*. TCL, IB, and IP: total cell lysate, immunoblotting, and immunoprecipitation, respectively. Arrows and arrowheads show the position of c-Src and TRAF6, respectively.

$Src^{-/-}$ pOCs on Vn, treated with IL-1, and found that anti-TRAF6 Abs did precipitate neither PYK2 nor $p130^{Cas}$ (Fig. 3*B*, *lanes 7–12*), suggesting that c-Src may play an important role in the association of PYK2 and $p130^{Cas}$ with TRAF6. IL-1-mediated association of TRAF6 and c-Src was further confirmed in OCLs, in which IL-1 induced the coimmunoprecipitation of c-Src with TRAF6, using anti-TRAF6 Abs (Fig. 4*A*, *lanes 1* and *2*). Furthermore, anti-c-Src polyclonal Abs reciprocally pulled down TRAF6 from IL-1-treated OCLs (Fig. 4*B*, *lane 1*). We also tried two different anti-c-Src mAbs only to fail to coprecipitate TRAF6 under the same condition (Fig. 4*B*, *lanes 2* and *3*), probably because these mAbs might interfere with the TRAF6 and Src association.

Intracellular localization of TRAF6 and c-Src in osteoclasts

Protein-protein interaction of TRAF6 and c-Src in osteoclasts led us to examining the intracellular localization of these molecules. Few actin rings were observed in purified OCLs that were seeded and serum starved for 4 h on glass coverslips (Fig. 5*Ba*). In these OCLs, c-Src and TRAF6 were distributed throughout the cytoplasm (Fig. 5*A*, *a* and *b*; *Bb*). However, when cells were treated with IL-1, both TRAF6 and c-Src were redistributed to the cell periphery, where they were colocalized (Fig. 5*Af*). Moreover, the ring-like distribution of TRAF6 at the cell periphery overlapped with that of F-actin (Fig. 5*Bf*), suggesting that TRAF6-Src complex may be involved in actin ring formation in osteoclasts.

An interesting phenomenon observed in this study was the translocation of TRAF6 to nucleus following IL-1 treatment (Fig. 5, *Ae* and *Be*), whereas c-Src was distributed only to perinuclear regions (Fig. 5*Ad*). As shown in Fig. 6*A*, TRAF6 started to traffic to nucleus 5 min after IL-1 treatment. The translocation of TRAF6 to nucleus and cell periphery seems to occur almost simultaneously. Furthermore, the translocation of

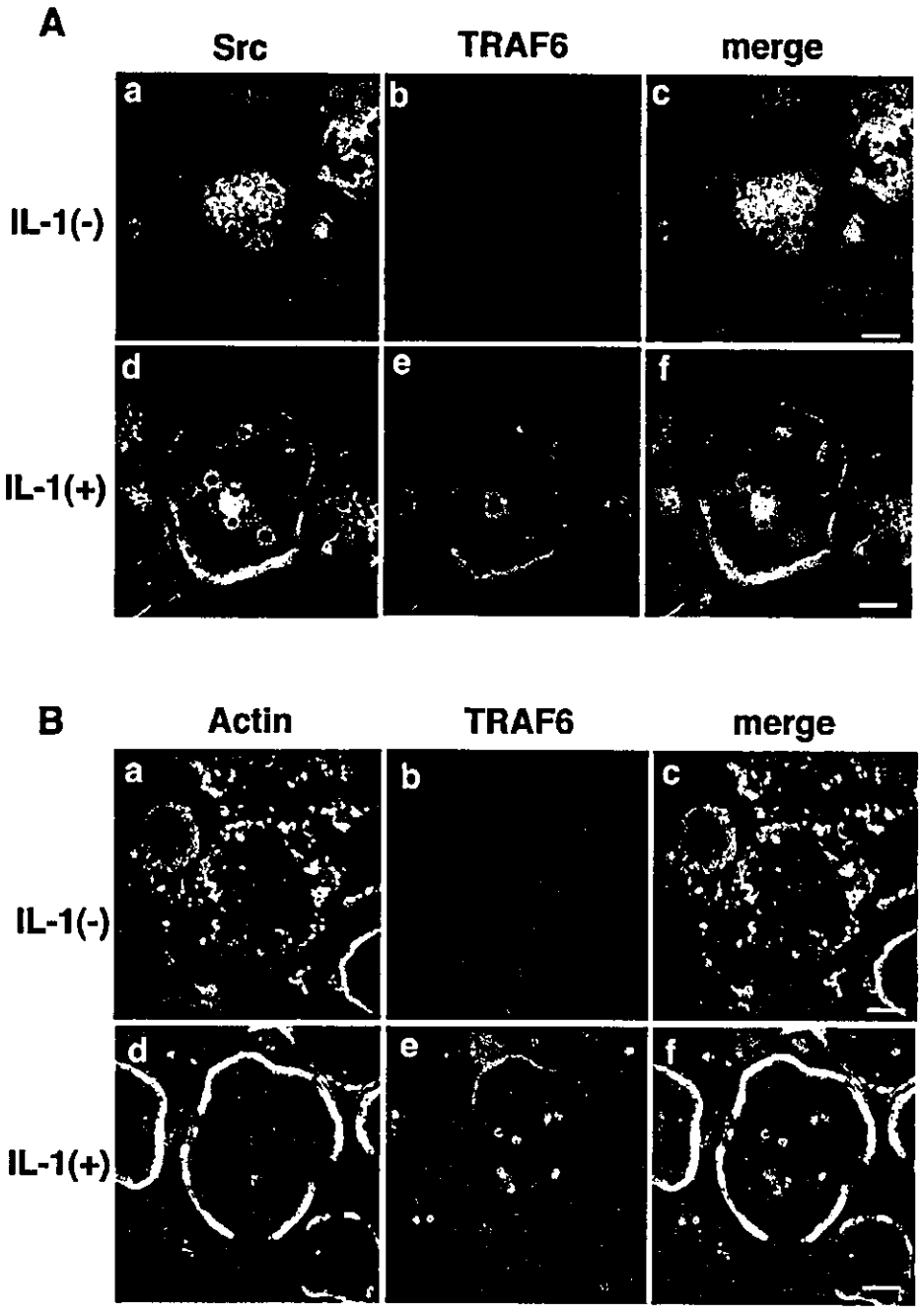

FIGURE 5. Effect of IL-1 on intracellular localization of TRAF6 in OCLs. Purified OCLs were prepared on glass coverslips, as described in *Materials and Methods*. After purification, cells were serum starved for 4 h, and then treated with (*A*, *d–f*, *B*, *d–f*) or without 10 ng/ml IL-1 (*A*, *a–c*; *B*, *a–c*) for 30 min. Cells were fixed and double immunostained for TRAF6 (*A*, *b* and *e*; *B*, *b* and *e*; red) and c-Src (*A*, *a* and *d*; green) or F-actin (*B*, *a* and *d*, green). Their colocalization is shown in yellow (*A*, *c* and *f*, *B*, *c* and *f*). Bars = 20 μm.

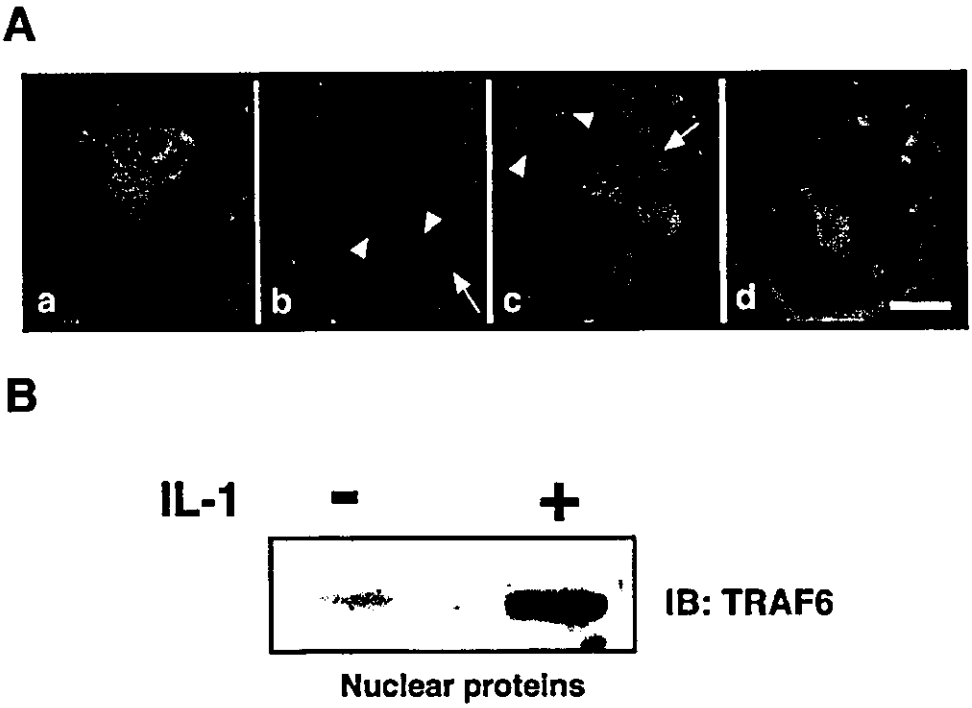

FIGURE 6. Effect of IL-1 on translocation of TRAF6 to nucleus in OCLs. *A*, Purified OCLs were prepared on glass coverslips, as described in *Materials and Methods*. After purification, cells were serum starved for 4 h, and then treated with 10 ng/ml IL-1 for 0 (*a*), 5 (*b*), 10 (*c*), and 30 (*d*) min. Cells were fixed and immunostained for TRAF6. Bars = 20 μm. *B*, Purified OCLs were serum starved for 4 h, and then treated with or without IL-1 (10 ng/ml) for 30 min. Nuclear proteins, prepared as described in *Materials and Methods*, were immunoblotted with anti-TRAF6 Ab. IB, immunoblotting.

TRAF6 to nucleus was also confirmed biochemically, as shown in Fig. 6*B*.

Discussion

In the previous study, we have shown that IL-1 is an important cytokine for osteoclastic bone resorption (10). In this study, therefore, we examined the mechanism of IL-1-induced osteoclast activation and the involvement of c-Src in IL-1 signal transduction in the regulation of osteoclast function. Using $Src^{+/?}$ and $Src^{-/-}$ osteoclast-like cells, we first demonstrated that c-Src is required for IL-1-induced tyrosine phosphorylation of $p130^{Cas}$, which was previously shown to take part in actin ring formation in osteoclasts in vitro (23). Second, we showed that IL-1 induces the complex formation of TRAF6, an adapter molecule for IL-1 signaling, c-Src, PYK2, and $p130^{Cas}$ in osteoclasts. c-Src is, also in this case, required for formation of this heteromeric complex, because IL-1 treatment of Src-deficient pOCs did not result in the association of TRAF6 with PYK2 and $p130^{Cas}$. Third, IL-1 induced the colocalization of TRAF6 and c-Src in the ring-like structures at the periphery of spreading osteoclasts. These ring structures also contained F-actin, a prerequisite for sealing zone formation during osteoclast activation (29). Our previous studies have documented the important role of c-Src and its association with PYK2 and $p130^{Cas}$ in the maintenance of the ring structure of F-actin (actin rings) and bone resorption (22, 24). Data presented in this work, therefore, might clarify another interesting role of c-Src as a transducer of IL-1 signaling to tyrosine phosphorylation pathway, leading to cytoskeletal reorganization and osteoclast activation.

These findings also support the in vivo findings showing that targeted disruption of either c-Src or TRAF6 in mice results in a similar osteopetrotic phenotype, caused by osteoclast dysfunction without change in osteoclast number (16, 17). In contrast, Naito et al. (30) reported that TRAF6 is an essential transducer for osteoclast differentiation, because TRAF6-deficient mice are defective in osteoclast formation and exhibit severe osteopetrosis. Although TRAF6 may be involved in both osteoclast differentiation and osteoclast function, in this study, we focused on the role of TRAF6 in osteoclast function.

During the course of this study, Wong et al. (31) reported that RANK ligand (TNF-related activation-induced cytokine/osteoclast differentiation factor/osteoprotegerin ligand), a TNF family member that stimulates osteoclast differentiation and function, activates Akt/protein kinase B through a signaling complex that includes TRAF6 and c-Src. In their study, the significance of this TRAF6-Src complex lies in RANK ligand-induced cell survival through the activation of Akt/protein kinase B, whereas our data suggest that this molecular complex is involved in the IL-1-induced cytoskeletal rearrangement and osteoclast activation via c-Src-mediated tyrosine phosphorylation of PYK2 and $p130^{Cas}$. Wong et al. also showed the direct interaction of TRAF6 and c-Src mediated by the RPTIPRNPK motif (aa 469–477) in TRAF6 and the Src homology 3 (SH3) domain in c-Src. The findings obtained to date and previous reports including ours suggest the sequence of the heteromeric molecular complex containing TRAF6, c-Src, PYK2, and $p130^{Cas}$, as follows: 1) association of TRAF6 and c-Src, mediated by the RPTIPRNPK motif in TRAF6 and the SH3 domain in c-Src (31); 2) interaction of c-Src and PYK2, mediated by the SH2 domain in c-Src and phosphotyrosine in PYK2 (22); 3) constitutive association of PYK2 and $p130^{Cas}$, mediated by proline-rich regions in PYK2 and an SH3 domain in $p130^{Cas}$ (24, 32). This study points to the significance of the TRAF6 and c-Src interaction in osteoclast activation and presents evidence for cross-talk between IL-1 signaling and tyrosine kinase pathways. In contrast, previous reports have demonstrated that IL-1-mediated cytosolic and nuclear signaling pathways require appropriate assembly of

cell-matrix adhesion complexes and organization of actin cytoskeleton (33–35). Therefore, we cannot rule out the possibility that the molecular complex, including TRAF6, c-Src, p130^{Cas}, and PYK2, shown in this work is indirectly involved in IL-1 signaling.

An additional novel observation reported in this study is the intracellular localization of TRAF6 in osteoclasts. Before IL-1 stimulation, TRAF6 is distributed throughout the cytoplasm; IL-1 induces a redistribution of TRAF6 to the cell periphery, where TRAF6 is colocalized with c-Src and F-actin. We have previously reported that both p130^{Cas} and PYK2 colocalize to the ring-like structure of F-actin (24). The biochemical and morphological evidence presented in this study suggests the involvement of a complex containing TRAF6, c-Src, PYK2, and p130^{Cas} in actin ring formation, leading to osteoclast activation by IL-1. We find in this study, using both morphological and biochemical methods, that upon IL-1 treatment, TRAF6 translocates also to the nucleus. IL-1 thus appears to induce translocation of TRAF6 into two subcellular localizations in osteoclasts, coincident with cell spreading: one pool of TRAF6 that localizes to actin rings in a c-Src-dependent manner, and the other that translocates to the nucleus. The requirement of c-Src for TRAF6 nuclear translocation remains unclear, because IL-1 treatment did not induce cell spreading and actin ring formation in Src-deficient osteoclasts. Biochemical analyses of TRAF6 translocation into the nuclear fraction of Src-deficient cells under treatments with various cytokines will be a subject of our future study. In addition, while TRAF4 was also reported to localize to cell nuclei (36), the physiological significance of these two cellular localizations of TRAF6 induced by cytokines requires further study.

In summary, we show that IL-1 induces, in Src-dependent manner, tyrosine phosphorylation of PYK2 and p130^{Cas}, known downstream mediators of the adhesion-dependent signaling pathway. Furthermore, IL-1 regulates the tyrosine kinase pathway, possibly by inducing the association of TRAF6 and c-Src, leading to further recruitment of PYK2 and p130^{Cas}. Finally, IL-1 induces osteoclast spreading and physical recruitment of the TRAF6/Src-dependent complex to the actin ring adhesion structures, a prerequisite for sealing zone formation, essential for osteoclast activation.

Acknowledgments

We thank Drs. Ai-ichiro Yamamoto, Toshiki Miura, Toru Akiyama, and Toru Ogata (University of Tokyo) for fruitful suggestions.

References

1. Dinarello, C. A. 1994. The interleukin-1 family: 10 years of discovery. *FASEB J. 8:1314.*
2. Gowen, M., D. D. Wood, E. J. Ihrie, M. K. B. Mcguire, and R. G. G. Russell. 1983. An interleukin-1-like factor stimulates bone resorption in vitro. *Nature 306:378.*
3. Boyce, B. F., T. B. Aufdemorte, I. R. Garrett, A. J. P. Yates, and G. R. Mundy. 1989. Effects of interleukin-1 on bone turnover in normal mice. *Endocrinology 125:1142.*
4. Lorenzo, J. A., S. L. Sousa, C. Alender, L. G. Raisz, and A. Dinarello. 1987. Comparison of the bone-resorbing activity in the supernatants from phytohemagglutinin-stimulated human peripheral blood mononuclear cells with that of cytokines through the use of an antiserum to interleukin 1. *Endocrinology 121:1164.*
5. Seckinger, P., J. Klein-Nulend, C. Alender, R. C. Thompson, J.-M. Dayer, and L. G. Raisz. 1990. Natural and recombinant human IL-1 receptor antagonists block the effects of IL-1 on bone resorption and prostaglandin production. *J. Immunol. 145:4181.*
6. Kimble, R. B., J. L. Vannice, D. C. Bloedow, R. C. Thompson, W. Hopfer, V. T. Kung, C. Brownfield, and R. Pacifici. 1994. Interleukin-1 receptor antagonist decreases bone loss and bone resorption in ovariectomized rats. *J. Clin. Invest. 93:1959.*
7. Suda, T., N. Takahashi, N. Udagawa, E. Jimi, M. T. Gillespie, and T. J. Martin. 1999. Modulation of osteoclast differentiation and function by the new members of the tumor necrosis factor receptor and ligand families. *Endocr. Rev. 20:345.*
8. Teitelbaum, S. L. 2000. Bone resorption by osteoclasts. *Science 289:1504.*
9. Akatsu, T., N. Takahashi, N. Udagawa, K. Imamura, A. Yamaguchi, K. Sato, N. Nagata, and T. Suda. 1991. Role of prostaglandins in interleukin-1-induced bone resorption in mice in vitro. *J. Bone Miner. Res. 6:183.*
10. Jimi, E., I. Nakamura, L. T. Duong, T. Ikebe, N. Takahashi, G. A. Rodan, and T. Suda. 1999. Interleukin-1 induces multinucleation and bone-resorbing activity of osteoclasts in the absence of osteoblasts/stromal cells. *Exp. Cell Res. 247:84.*
11. Thomson, B. M., J. Saklatvala, and T. J. Chambers. 1986. Osteoblasts mediate interleukin 1 stimulation of bone resorption by rat osteoclasts. *J. Exp. Med. 164:104.*
12. Jimi, E., T. Shuto, and T. Koga. 1995. Macrophage colony-stimulating factor and interleukin-1α maintain the survival of osteoclast-like cells. *Endocrinology 136:808.*
13. Jimi, E., I. Nakamura, T. Ikebe, S. Akiyama, N. Takahashi, and T. Suda. 1998. Activation of NF-κB is involved in the survival of osteoclasts promoted by interleukin-1. *J. Biol. Chem. 273:8799.*
14. Miyazaki, T., H. Katagiri, Y. Kanegae, H. Takayanagi, Y. Sawada, A. Yamamoto, M. P. Pando, T. Asano, I. M. Verma, H. Oda, et al. 2000. Reciprocal role of ERK and NF-κB pathways in survival and activation of osteoclasts. *J. Cell Biol. 148:333.*
15. Kopp, E. B., and R. Medzhitov. 1999. The Toll-receptor family and control of innate immunity. *Curr. Opin. Immunol. 11:13.*
16. Lomaga, M. A., W.-C. Yeh, I. Sarosi, G. S. Duncan, C. Furlonger, A. Ho, S. Morony, C. Capparelli, G. Van, S. Kaufman, et al. 1999. TRAF6 deficiency results in osteopetrosis and defective interferkin-1, CD40, and LPS signaling. *Genes Dev. 13:1015.*
17. Soriano, P., C. Montgomery, R. Geske, and A. Bradley. 1991. Targeted disruption of the c-*src* proto-oncogene leads to osteopetrosis in mice. *Cell 64:693.*
18. Boyce, B. F., T. Yoneda, C. Lowe, P. Soriano, and G. R. Mundy. 1992. Requirement of pp60$^{c\text{-}src}$ expression for osteoclasts to form ruffled border and resorb bone in mice. *J. Clin. Invest. 90:1622.*
19. Wesolowski, G., L. T. Duong, P. T. Lakkakorpi, R. M. Nagy, K. Tezuka, H. Tanaka, G. A. Rodan, and S. B. Rodan. 1995. Isolation and characterization of highly enriched, prefusion mouse osteoclastic cells. *Exp. Cell Res. 219:679.*
20. Suda, T., E. Jimi, I. Nakamura, and N. Takahashi. 1997. Role of 1α,25-dihydroxyvitamin D_3 in osteoclast differentiation and function. In *Methods in Enzymology: Vitamins and Coenzymes*, Vol. 282. D. B. McCormick, J. W. Suttie, and C. Wagner, eds. Academic Press, San Diego, pp. 223.
21. Kobayashi, K., N. Takahashi, E. Jimi, N. Udagawa, M. Takami, S. Kotake, N. Nakagawa, M. Kinosaki, K. Yamaguchi, N. Shima, et al. 2000. Tumor necrosis factor α stimulates osteoclast differentiation by a mechanism independent of the ODF/RANKL-RANK interaction. *J. Exp. Med. 191:275.*
22. Duong, L. T., P. T. Lakkakorpi, I. Nakamura, M. Machwate, R. M. Nagy, and G. A. Rodan. 1998. PYK2 in osteoclasts is an adhesion kinase, localized in the sealing zone, activated by ligation of $\alpha_v\beta_3$ integrin, and phosphorylated by Src kinase. *J. Clin. Invest. 102:881.*
23. Nakamura, I., E. Jimi, L. T. Duong, T. Sasaki, N. Takahashi, G. A. Rodan, and T. Suda. 1998. Tyrosine phosphorylation of p130^{Cas} is involved in actin organization in osteoclasts. *J. Biol. Chem. 273:11144.*
24. Lakkakorpi, P. T., I. Nakamura, R. M. Nagy, J. T. Parsons, G. A. Rodan, and L. T. Duong. 1999. Stable association of PYK2 and p130^{Cas} in osteoclasts and their co-localization in the sealing zone. *J. Biol. Chem. 274:4900.*
25. Nakamura, I., L. Lipfert, G. A. Rodan, and L. T. Duong. 2001. Convergence of $\alpha_v\beta_3$ integrin- and M-CSF-mediated signals in osteoclasts: the involvement of phospholipase-Cγ. *J. Cell Biol. 152:361.*
26. Hamasaki, K., T. Mimura, N. Morino, H. Furuya, T. Nakamoto, S. Aizawa, C. Morimoto, Y. Yazaki, H. Hirai, and Y. Nojima. 1996. Src kinase plays an essential role in integrin-mediated tyrosine phosphorylation of Crk-associated substrate p130^{Cas}. *Biochem. Biophys. Res. Commun. 222:338.*
27. Vuori, K., H. Hirai, S. Aizawa, and E. Ruoslahti. 1996. Induction of p130^{Cas} signaling complex formation upon integrin-mediated cell adhesion: a role for Src family kinases. *Mol. Cell. Biol. 16:2606.*
28. Cao, Z., J. Xiong, M. Takeuchi, T. Kurama, and D. V. Goeddel. 1996. TRAF6 is a signal transducer for interleukin-1. *Nature 383:443.*
29. Nakamura, I., N. Takahashi, T. Sasaki, E. Jimi, T. Kurokawa, and T. Suda. 1996. Chemical and physical properties of the extracellular matrix are required for actin ring formation in osteoclasts. *J. Bone Miner. Res. 11:1873.*
30. Naito, A., S. Azuma, S. Tanaka, T. Miyazaki, S. Takaki, K. Takatsu, K. Nakao, K. Nakamura, M. Katsuki, T. Yamamoto, and J. Inoue. 1999. Severe osteopetrosis, defective interleukin-1 signalling and lymph node organogenesis in TRAF6-deficient mice. *Genes Cells 4:353.*
31. Wong, B. R., D. Besser, N. Kim, J. R. Arron, M. Vologodskaia, H. Hanafusa, and Y. Choi. 1999. TRANCE, a TNF family member, activates Akt/PKB through a signaling complex involving TRAF6 and c-Src. *Mol. Cell 4:1041.*
32. Ohba, T., M. Ishino, H. Aoto, and T. Sasaki. 1998. Interaction of two proline-rich sequences of cell adhesion kinase β with SH3 domains of p130^{cas}-related proteins and a GTPase-activating protein, Graf. *Biochem. J. 330:1249.*
33. Arora, P. D., J. Ma, W. Min, T. Cruz, and C. A. G. McCulloch. 1995. Interleukin-1 induced calcium flux in human fibroblasts is mediated through focal adhesions. *J. Biol. Chem. 270:6042.*
34. Lo, Y. Y., L. Luo, C. A. McCulloch, and T. F. Cruz. 1998. Requirements of focal adhesions and calcium fluxes for interleukin-1-induced ERK kinase activation and c-*fos* expression in fibroblasts. *J. Biol. Chem. 273:7059.*
35. MacGillivray, M. K., T. F. Cruz, and C. A. McCulloch. 2000. The recruitment of the interleukin-1 (IL-1) receptor-associated kinase (IRAK) into focal adhesion complexes is required for IL-1β-induced ERK activation. *J. Biol. Chem. 275:23509.*
36. Régnier, C. H., C. Tomasetto, C. Moog-Lutz, M.-P. Chenard, C. Wendling, P. Basset, and M.-C. Rio. 1995. Presence of a new conserved domain in CART1, a novel member of the tumor necrosis factor receptor-associated protein family, which is expressed in breast carcinoma. *J. Biol. Chem. 270:25715.*

ELSEVIER

Atherosclerosis 162 (2002) 323-334

ATHEROSCLEROSIS

www.elsevier.com/locate/atherosclerosis

Large scale isolation of non-uniform shear stress-responsive genes from cultured human endothelial cells through the preparation of a subtracted cDNA library

Hajime Yoshisue [a], Keiko Suzuki [a], Ayako Kawabata [a], Takeshi Ohya [b], Hanjun Zhao [b], Kazuhiro Sakurada [a], Yoji Taba [c], Toshiyuki Sasaguri [c], Naohiko Sakai [b], Shizuya Yamashita [b], Yuji Matsuzawa [b], Hiroshi Nojima [d,*]

[a] *Tokyo Research Laboratories, Kyowa Hakko Kogyo Co., Ltd., 3-6-6 Asahi-machi, Machida, Tokyo 194-8533, Japan*
[b] *Department of Internal Medicine and Molecular Science, Graduate School of Medicine, Osaka University, 2-2 Yamadaoka, Suita, Osaka 565-0871, Japan*
[c] *Department of Bioscience, National Cardiovascular Center Research Institute, 5-7-1 Fujishiro-dai, Suita, Osaka 565-8565, Japan*
[d] *Department of Molecular Genetics, Research Institute for Microbial Diseases, Osaka University, 3-1 Yamadaoka, Suita City, Osaka 565-0871, Japan*

Received 10 May 2001; received in revised form 20 September 2001; accepted 8 October 2001

Abstract

To investigate the molecular mechanisms responsible for the regional selectivity of early atherogenesis, we have applied a non-uniform shear stress to cultured human umbilical vein endothelial cells (HUVEC). We used a microcarrier culture system and a combination of subtraction and reverse-subtraction methods to isolate a number of genes upregulated by shear stress. The resultant subtracted library includes several known genes (e.g. MCP-1, TM) whose responsiveness to shear stress has been previously reported, indicating that the library is enriched for genes upregulated by shear stress. Also included are atherosclerosis-related genes (e.g. CTGF, IL-8) whose responsiveness to shear stress had not been demonstrated, other known genes whose relationship to atherosclerosis had not been reported, and novel genes. Some responsive to centrifugal force and shear stress (*RECS*) genes are also upregulated following stimulation by steady laminar shear stress in a parallel plate chamber. Interestingly, the library includes ET-1 and PAI, which are well known atherogenic factors that are downregulated by laminar shear stress. This implies that turbulent shear stress has effects on HUVEC that are different from those elicited by laminar shear stress. Importantly, analysis of specimens taken from human aorta showed that several *RECS* genes are transcriptionally upregulated in atherosclerotic lesions, suggesting that the subtracted library includes novel therapeutic targets for the treatment of atherosclerosis.

Keywords: Shear stress; Vascular endothelial cell; Atherogenic; Subtraction

1. Introduction

Many studies have shown that vascular endothelium, the single-cell lining of the vasculature, plays a pivotal role in the normal functioning of the cardiovascular system, and that endothelial dysfunction can be associated with the development of disease, especially atherosclerosis. Due to their unique location, endothelial cells are dynamically exposed to a variety of biochemical substances contained in blood and are responsive to many of these substances, some of which are necessary for vascular homeostasis, and others which (e.g. cholesterol and oxidized LDL) can be risk factors for atherogenesis at elevated plasma concentrations [1]. Despite the presence of these systemic risk factors, early atherosclerotic lesions are not randomly distributed but are limited to specific regions of arterial walls, such as branch points and curvatures, which are

* Corresponding author. Tel.: +81-6-6875-3980; fax: +81-6-6875-5192.
E-mail address: hnojima@biken.osaka-u.ac.jp (H. Nojima).

0021-9150/02/$ - see front matter
PII: S0021-9150(01)00735-3

areas that experience chaotic and non-uniform blood flow. In contrast, early lesions are generally absent from more linear regions, where steady and streamlined flow occurs. These observations have been reported not only for experimental animals but also for humans and suggest that hemodynamic forces are involved in the initiation and localization of early atherogenesis [2]. Among biomechanical stimuli, shear stress, which is a dragging force generated by blood flow and viscosity, appears to be especially important, because it directly provokes physiological alterations in endothelial cells, many of which are associated with changes in gene expression [3,4]. From numerous investigations it is now clear that endothelial cells can sense and respond to shear stress. It is therefore possible that endothelial cells in vivo respond differentially to their local hemodynamic environment, so that phenotypic changes in these cells are involved in early atherogenesis. Although the molecular mechanism by which shear stress is involved in the initiation of atherosclerosis has not been clarified, a number of studies using an in vitro flow apparatus have shown that steady laminar shear stress induces cellular responses that are essential for the atheroprotective functions of endothelial cells [5–7]. For example, the production of NO, a vasodilator critical for atheroprotection, rapidly increases upon stimulation by laminar shear stress, due to a rapid activation of the endothelial isoform of nitric oxide synthase (ecNOS) [6]. A recent report by Topper et al. indicated that the ecNOS mRNA is upregulated by laminar flow but not by turbulent flow [7]. They also showed that other atheroprotective genes, such as those encoding cyclooxygenase (COX)-2 and manganese-dependent superoxide dismutase (Mn-SOD), demonstrate a laminar shear stress-selective pattern of induction [7]. A growing number of physiologically or pathophysiologically important endothelial genes have been reported to respond to fluid stimulation, leading to a general paradigm that atheroprotective genes are upregulated and atherogenic genes are downregulated by laminar shear stress [3,4]. Examples of downregulated atherogenic molecules are vascular cell adhesion molecule (VCAM)-1 [8] and prepro-endothelin (ET)-1 [9]. There are exceptions, however, such as atherogenic intercellular adhesion molecule-1, which is more clearly upregulated by laminar shear stress than by turbulent shear stress [7], and thrombomodulin (TM), an antithrombotic factor, which is upregulated by turbulent shear stress as well as by laminar shear stress [4,10]. Furthermore, TM has also been reported to be downregulated by laminar shear stress [11]. Thus, the relationship between the functions of these genes and their expression profiles, as modulated by flow patterns, is not clear-cut.

We have recently reported a highly efficient method for subtraction cloning [12]. In the present study, we have used our method to identify a comprehensive list of endothelial genes that are upregulated by non-uniform shear stress, certain of which could be novel candidates for genes implicated in atherogenesis.

2. Materials and methods

2.1. Cell culture

Human umbilical vein endothelial cells (HUVEC) were purchased from Clonetics (San Diego, CA) and propagated in F-12K medium (Dainippon Pharmaceutical, Japan) supplemented with 100 μg/ml heparin, 30 μg/ml endothelial cell growth supplement (Beckton Dickinson, Flanklin Lakes, NJ), and 10% fetal calf serum (FCS) in tissue culture plastic flasks precoated with 2 mg/ml gelatin. Cells were routinely passaged with 0.05% trypsin/2 mM EDTA in phosphate buffered saline (PBS). Cells of up to the fifteenth passage were used in shear stress experiments.

2.2. Shear stress apparatus

Non-uniform shear stress was induced by microcarrier culture in a modification of the method of Cooke et al. [13]. Then 2×10^6 of HUVEC were scraped from the dishes, washed in PBS, and suspended with 2 g of Cytodex 3 microcarrier beads (Amersham Pharmacia Biotech, Uppsala, Sweden) in 35 ml of F-12K medium. The suspension was transferred to a spinner flask with a volume of nearly 200 ml and a diameter of 6 cm. The flask contained a stir bar and was mounted on a magnetic stirrer. After microscopic observation to confirm that the HUVEC had attached to the surfaces of the microcarrier beads, the stirrer was activated at a rotation speed of 160 rpm to induce a vortical flow. The lengths of the periods of rotation were 0 (without shear stress), 0.5, 1, 1.5, 2, 3, 4, 6, 10, or 20 h. Cells remained attached to the beads even after 20 h of stimulation, indicating that the flow forces generated in the flask are likely within physiological ranges. Experiments of steady laminar shear stress were performed using a parallel-plate flow chamber as described previously [14].

2.3. Isolation of RNA

Total cellular RNA was isolated as reported previously [12]. One hundred micrograms of total RNA were prepared from HUVEC subjected to shear stress for each of nine different periods were pooled, and the resultant 900 μg of total RNA was passed through an oligo(dT)-cellulose chromatography column (Collaborative Biomedical Products, Bedford, MA) for the purification of poly(A)$^+$ RNA.

2.4. RT-PCR analysis

cDNAs were synthesized from 1 μg of total RNA with the SuperScript Preamplification System (Gibco BRL, Rockville, MD), and one fortieth of the cDNA product was used in each reaction. PCR reactions were done on a Gene Amp PCR System 9600 (Perkin–Elmer, Norwalk, CT). For the analysis of laminar flow-dependent expression, the PCR products were subjected to electrophoresis and stained by SYBR Green I (Takara Shuzo, Kyoto, Japan), and the intensity of the fragments was quantified with a FluorImager (Molecular Dynamics, Sunnyvale, CA). The specific primers used are shown in Table 1.

2.5. Construction of the subtracted cDNA library

A cDNA library was generated from 3 μg of poly(A)$^+$ RNA from HUVEC subjected to shear stress, by the method of Kobori et al. [12]. Subtraction procedures are as described earlier [12] except that 20 μg photobiotinylated poly(A)$^+$ RNA from HUVEC not subjected to shear stress was hybridized with 0.5 μg single-stranded DNA from the cDNA library prepared from shear-stressed HUVEC.

Table 1
Oligonucleotide sequences used for PCR

Gene name	DNA strand	Nucleotide sequences
t-PA	Sense	5′-CTGCAGCTGAAATCGGATTCGT-3′
	Antisense	5′-CTGATGATGCCCACCAAAGTC-3′
Thrombomodulin	Sense	5′-CTCATAGGCATCTCCATCGCG-3′
	Antisense	5′-CCGCGCACTTGTACTCCATCT-3′
PDGF-A	Sense	5′-GTCCGCCAACTTCCTGATCTGG-3′
	Antisense	5′-ATTCAGGCTTGTGGTCGCGCAG-3′
G3PDH	Sense	5′-CCCATCACCATCTTCCAGGAGC-3′
	Antisense	5′-TTCACCACCTTCTTGATGTCATCATA-3′
RECS1	Sense	5′-CACCTACTGTATGACACCACATTC-3′
	Antisense	5′-GAGATGCTGTTCCATGCTGGCCTG-3′
RECS10	Sense	5′-TGGCATCTTCTTATGCTTCTAGTG-3′
	Antisense	5′-TACAATGTAGATGTCTTGGCGACC-3′
RECS12	Sense	5′-AAAAGAACCGGATGCAGCTTTCGG-3′
	Antisense	5′-GCTCTCCATGCCTCAGATTATCTC-3′
RECS26′	Sense	5′-TGTTATGTACCTGCATCACGTTGG-3′
	Antisense	5′-CACGGCTTCACGTTTCTGCTTTG-3′

2.6. Reverse subtraction

After four cycles of subtraction, the subtracted library was converted into single stranded DNA using the helper phage R408. Two micrograms of photobiotinylated poly(A)$^+$ RNA from HUVEC exposed to shear stress were incubated with 2 μg single-stranded DNA at 42 °C for 48 h in 25 μl hybridization solution [12]. Four hundred microliters of a solution containing 50 mM HEPES (pH 7.5), 2 mM EDTA, and 500 mM NaCl, and 14 μg of streptavidin (Gibco BRL) were added to the hybridization mixture, followed by incubation at room temperature for 5 min. After three rounds of phenol/chloroform treatment, the aqueous phase containing single-strand DNA was removed. Four hundred microliters of TE was added to the organic phase, which contained the single-stranded DNA complexed with poly(A)$^+$ RNA. The solution was heated at 95 °C for 5 min and then chilled on ice to denature the hybrids. The aqueous phase, which now included the single-strand DNA that had been released from the poly(A)$^+$ RNA, was collected and applied to a microfilter (UFCP3LTK50, Millipore, Bedford, MA) to be concentrated. Afterwards, the single-strand DNA was converted into the double-strand form by a previously described method [12], followed by transformation into the *E. coli* strain MC1061A.

2.7. Northern blot analysis

Four micrograms of total RNA from shear-stressed or unstressed HUVEC were electrophoresed through a 1% agarose gel containing formaldehyde and MOPS, and transferred onto a Biodyne A nylon membrane (PALL Biosupport, East Hills, NY). Northern hybridization was performed by a previously described method [12].

2.8. DNA sequencing and homology search

Dideoxy-chain termination sequencing reactions were performed using the BigDye Terminator Cycle Sequencing Ready Reaction Kit (Perkin–Elmer), and the reaction products were analyzed by a 377 DNA sequencer (Perkin–Elmer). Sequences were compared by BLAST analysis with the GenBank, EMBL, and EST databases, as well as the human UniGene cluster database.

2.9. Isolation of full-length cDNAs

A cDNA library was constructed from 4 μg of poly(A)$^+$ RNA from shear-stressed HUVEC using a

ZAP-cDNA synthesis Kit (Stratagene, La Jolla, CA), according to the method described in the manufacturer's manual. A digoxigenin-labeled cDNA probe corresponding to each responsive to centrifugal force and shear stress (*RECS*) clone was synthesized using a PCR digoxigenin labeling mix (Hoffmann-LaRoche, Basel, Switzerland) and used for plaque hybridization.

2.10. Analysis of the expression of RECS genes in the human aorta

Aortic tissue was obtained by autopsy from a single patient. Specimens were taken from the non-sclerotic aortic arch and from the abdominal aorta near the bifurcation of the common iliac arteries, which exhibited advanced atherosclerosis. Total RNA was extracted with Sepasol-RNA solution (Nacalai Tesque, Kyoto, Japan). Northern hybridization was done according to the method described above.

3. Results

3.1. Evaluation of the experimental system

Since our objective was to isolate candidate genes involved in the formation of lesions in early atherosclerosis, we reasoned that a non-uniform fluid flow would be more suitable for finding genes implicated in atherogenesis than the laminar flow that is used in most shear stress-related work. Thus, we used a microcarrier culture system that exposes cells to turbulent rather than laminar shear stress. In this system, the pattern of flow is vortical, in contrast to the laminar flow produced by parallel-plate or cone-plate chambers. First, we tested whether shear stress was actually experienced by HUVEC in our culture conditions by examining the expression of known shear stress-responsive genes. Semiquantitative RT-PCR analysis showed that the levels of intracellular mRNA of representative shear stress-responsive genes, such as tissue-type plasminogen activator (tPA), platelet-derived growth factor (PDGF)-A and TM, clearly increase upon exposure to turbulent flow (Fig. 1). The kinetics of expression of these genes is similar to what has been previously reported, in that tPA is upregulated at later times [15], PDGF-A is expressed transiently at earlier times [16], and TM shows a sustained increase in expression [10] from 2 to 20 h. Although laminar shear stress was utilized to stimulate HUVEC in all previous studies of these three genes, the reported data are consistent with our results because several genes, such as PDGF-A, PDGF-B, and TM, respond similarly to laminar and turbulent flow [4,7,11]. On the other hand, the C-type natriuretic peptide mRNA, which had been reported to be upregulated by laminar shear stress [17], could not be detected

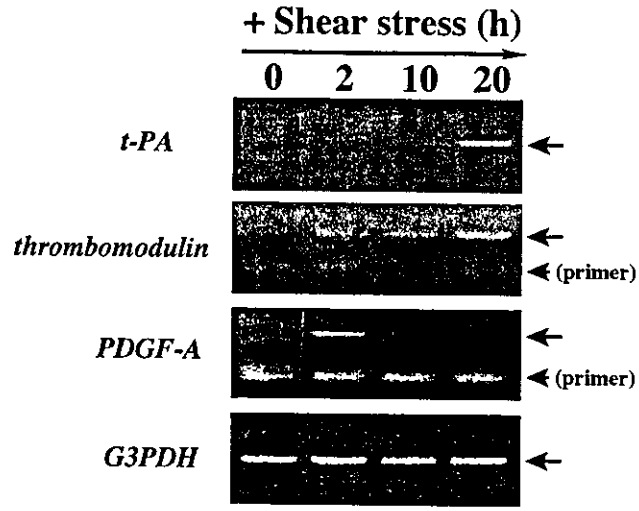

Fig. 1. Upregulation of known shear stress-responsive genes in HUVEC under non-uniform flow conditions. Semi-quantitative RT-PCR analysis was done as described in Section 2. The number of PCR cycles was 25 for t-PA, 30 for TM and PDGF-A, and 20 for G3PDH. For each gene, a representative result from three independent experiments is shown.

at any time during our culture conditions (data not shown), indicating that the profile of gene expression in HUVEC in our non-uniform flow conditions overlaps with, but is not identical to, that of HUVEC exposed to laminar flow conditions.

3.2. Identification of subtraction- and reverse subtraction-enriched genes upregulated by shear stress

We first prepared a subtracted cDNA library by carrying out four cycles of subtraction, using a method developed to isolate osteoclast-specific genes [12]. We used HUVEC subjected to shear stress as a tester and untreated cells as a driver. In the resultant library, S4, about 40% of the randomly picked clones contained very short cDNA inserts or no insert at all, probably because these clones were overrepresented due to multiple rounds of hybridization. In order to determine the success rate of the subtraction, 20 cDNA clones randomly selected from the S4 library were subjected to Northern analysis. We found that one clone demonstrates clear upregulation by shear stress, nine show no differential expression, and the other ten clones are not expressed (data not shown). This suggests that the subtraction was performed successfully, but clones that are expressed rarely in both tester and driver fractions, and which did not form hybrids, were overrepresented. To raise the frequency of the upregulated genes, we established a novel method of 'reverse subtraction'. The S4 library was hybridized with poly(A)$^+$ RNA from HUVEC subjected to shear stress, and hybridizing single-strand cDNAs were isolated and used to construct a

new version of the subtracted library, named S4R. We found that about 90% of randomly picked clones from S4R harbor insert DNAs, suggesting that the clones without inserts in S4 had been removed by reverse subtraction. Furthermore, specific signals for all 20 of the randomly selected inserted cDNAs from S4R could be detected by Northern analysis, among which five clones show clear upregulation by shear stress (see below). This result indicates that the rarely expressed genes in the S4 library were also eliminated, and consequently differentially regulated genes were concentrated by reverse subtraction. We used this S4R library to perform a comprehensive screen for upregulated genes.

3.3. RECS genes from the subtracted library

We randomly picked 500 independent clones from the S4R subtracted library, and subjected them to Northern analysis in order to select differentially regulated genes. Eighty-two of these clones proved to be upregulated by shear stress, and defined 63 independent genes on the basis of DNA sequence. Fig. 2 shows the Northern blot analysis of all shear stress-upregulated genes identified in this study, which we have called *RECS*. Since the RNA samples used in Fig. 2 are mixtures of samples taken at nine different time points (see Section 2), this type of screen would identify only those genes that are upregulated throughout the course

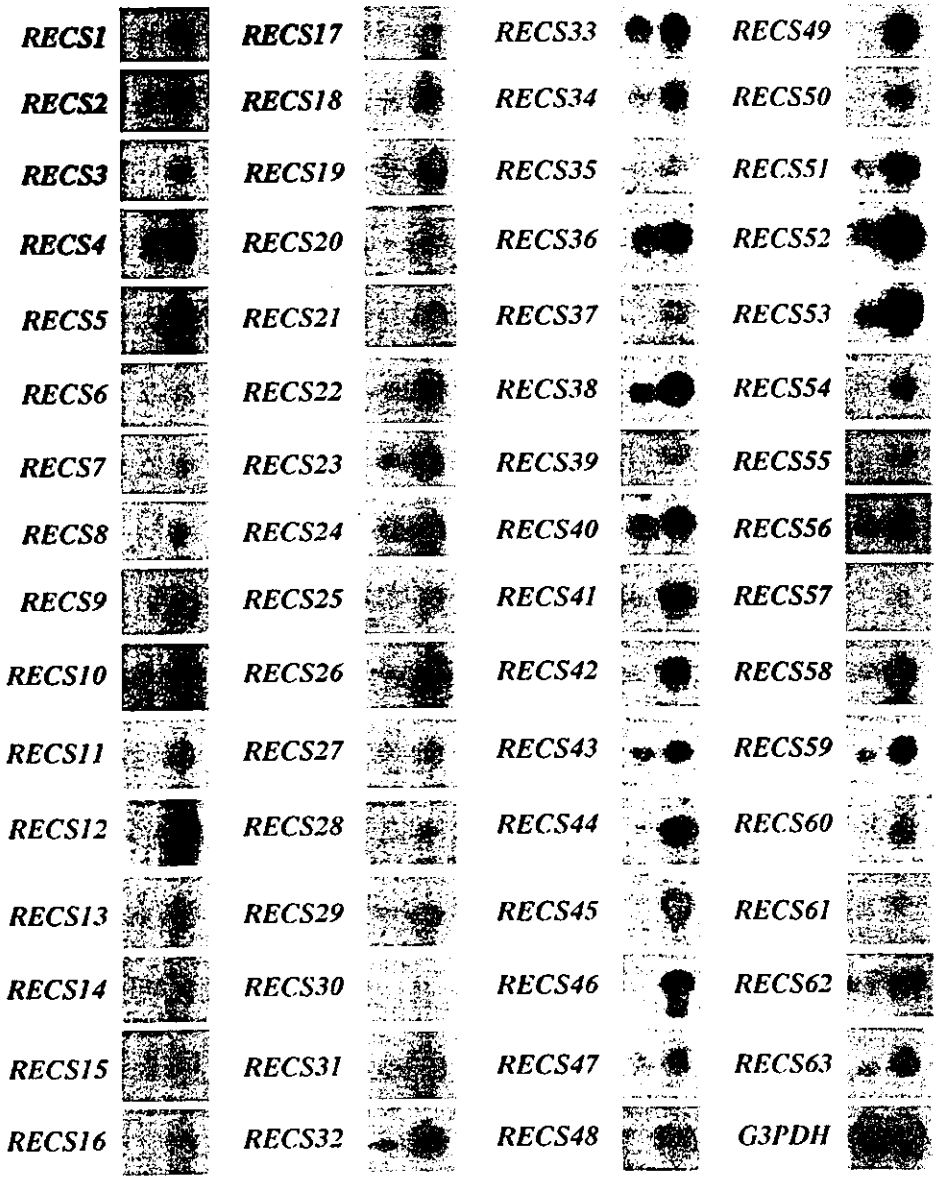

Fig. 2. Northern blot analysis of *RECS* genes. Total RNA from HUVEC stimulated with non-uniform flow in a spinner flask for nine different lengths of time was mixed in equal ratio, and 4 μg of the mixture were loaded in the right lane in each gel. Four micrograms of total RNA prepared from HUVEC on microcarrier beads not subjected to turbulent flow were loaded in the left lane.

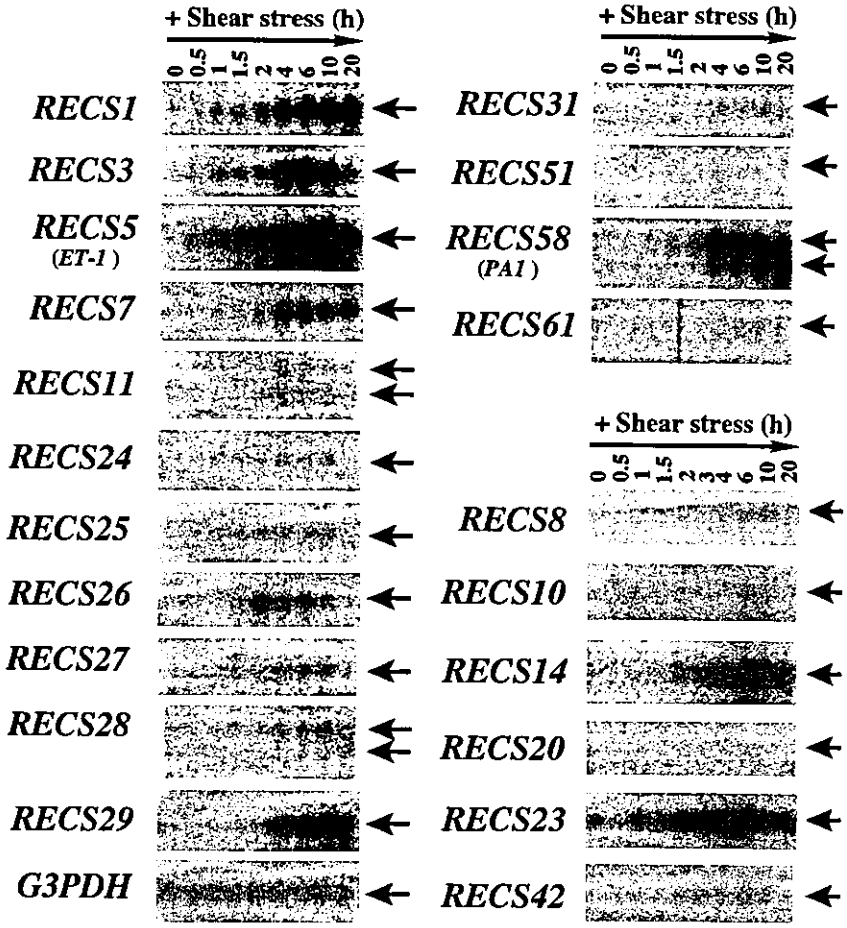

Fig. 3. Chronological expression of *RECS* genes. Four micrograms of total RNA prepared from HUVEC samples taken at 0, 0.5, 1, 1.5, 2, (3), 4, 6, 10 and 20 h after starting flow were loaded from left to right in each gel. Specific bands on each blot are indicated by arrows. G3PDH was used as a loading control.

of flow stimulation. In other words, transiently upregulated genes, like tPA and PDGF-A, might be missed. The timecourse of expression profiles does indeed show that most of the examined *RECS* genes are upregulated at almost all time points from 0.5 to 20 h (Fig. 3). The cognate identification or characteristics for the 63 genes is presented in Table 2. It should be noted that Table 2 includes several genes whose responsiveness to shear stress has been already reported: monocyte chemoattractant protein-1 (MCP-1; *RECS9*) [18], heparin-binding EGF-like growth factor (HB-EGF; *RECS33*) [19], laminin B1 (*RECS51*) [20], TM (*RECS55*) [10], transforming growth factor-β (TGF-β; *RECS56*) [21] and thrombospondin (*RECS62*) [4] are all upregulated by laminar shear stress. This is consistent with the result shown in Fig. 1, namely, many known laminar flow-upregulated genes are also upregulated by non-uniform flow in our culture conditions. The high frequency of detection of these clones serves as a positive control to indicate that the desired upregulated genes were enriched in the S4R library. Interestingly, ET-1 (*RECS5*), which was previously found to be downregulated by laminar shear stress [9], was the most frequent clone encountered (four times among the 82 clones; Table 2), and its mRNA level is dramatically increased upon stimulation by non-uniform flow (Fig. 3). Another notable clone is PAI-1 (*RECS59*), which was reported to be downregulated by laminar shear stress [22] or not to respond to it [23]. The difference in results is presumably due to experimental conditions, in that turbulent shear stress rather than steady laminar shear stress was applied to the cells. Furthermore, we found several genes which are atherosclerosis-related but have not been reported to be shear stress-responsive, such as connective tissue growth factor (CTGF; *RECS53*) and interleukin (IL)-8 (*RECS60*).

3.4. Full-length cloning of novel or functionally unknown RECS genes

Table 2 lists a number of genes whose functions have not been clarified, or whose full-length cDNAs have not been registered in the public databases. Given that many atherosclerosis-related genes are concentrated in

Table 2
List of shear stress-upregulated genes identified in the S4R subtracted cDNA library

Number[a]	mRNA size (kb)	Gene name	Accession	Frequency	Comments
Recs1	3.0	PP1201	NM_022152	1	FLC[b]
Recs2	2.2	EST (UniGene)	Hs.173840	1	FLC
Recs3	3.5	Thioredoxin reductase	X91247	1	
Recs4	1.8	LPS-induced protein gene	Q51544	1	
Recs5	3.5	Endothelin-1 precursor	J05008	4	RSS[c]
Recs6	3.3	Spliceosome-associated protein (SAP145)	U41371	1	
Recs7	4.3	AK023281	AK023281	1	FLC
Recs8	4.4	Puromycin-sensitive aminopeptidase	AJ132583	1	
Recs9	1.0	Monocyte chemotactic protein-1	S69738	1	RSS
Recs10	5.5	EST (UniGene)	Hs.5890	1	
Recs11	3.0	Lamin C	M13451	2	
Recs12	2.9	Cytokine-response gene CR8 (DEC1)	T43383	1	
Recs13	4.1	Human enhancer of filamentation (HEF1)	L43821	1	
Recs14	4.5	KIAA1029	AB028952	1	
Recs15	1.0	Interferon-induced 15-kDa protein gene	M21786	1	
Recs16	5.0	LDL receptor	N60388	1	
Recs17	4.0	EST	AW504157	1	
Recs18	1.7	Peripheral myelin protein (PMP)-22	Q32869	2	
Recs19	3.7	Tyrosine kinase receptor UFO/Ark	S65125	1	
Recs20	6.5	EST (UniGene)	Hs.112157	1	
Recs21	7.5	Calcium-ATPase HK2	M23115	1	
Recs22	1.1	Human arginine-rich protein	M83751	2	
Recs23	3.0	Human PR01110	A37031	3	FLC
Recs24	3.5	EST (UniGene)	Hs.121715	1	FLC
Recs25	4.2	BOG25	AF147747	1	FLC
Recs26	3.2	KIAA0025	D14695	3	
Recs27	3.2	High-mobility group phosphoprotein isoform I-C	U28749	2	
Recs28	3.0	Human Ras-like protein	X33415	1	
Recs29	3.0	Cyclin D1	X59798	2	
Recs30	4.0	KIAA0964, PSD-95/SAP90-associated protein-4	AB023181	1	
Recs31	2.7	Lamin A	M13452	1	
Recs32	2.0	CYR61/connective tissue growth factor-2	U62015	3	
Recs33	2.6	Heparin-binding EGF-like growth factor	M60278	1	RSS
Recs34	4.2	MIR16, membrane interacting protein of RGS16	AF212862	1	FLC
Recs35	1.8	Human homolog of the p64 bovine chloride channel	Y12696	1	
Recs36	1.2	Nicotinamide *N*-methyltransferase	U08021	2	
Recs37	6.0	EST	R07925	1	
Recs38	3.3	Surface glycoprotein	Z50022	1	
Recs39	3.5	Early growth response gene alpha (EGR-alpha)	S81439	1	
Recs40	3.0	Nuclear factor SF2p33	M69040	1	
Recs41	4.4	P66 shc	U73377	1	
Recs42	4.2	DKFZp564J0863	AL117600	1	FLC
Recs43	3.0	Lysosomal acid lipase (LAL)	M74775	1	
Recs44	3.0	N^G,N^G-dimethylarginine dimethylaminohydrolase	AB001915	1	
Recs45	3.5	EST (UniGene)	Hs.34160	1	
Recs46	3.0	Serum deprivation response (SDPR)	AF085481	1	
Recs47	3.7	EST (UniGene)	Hs.193974	1	
Recs48	6.0	AK021823	AK021823	1	
Recs49	2.0	Cytokine-inducible nuclear protein C-193	X83703	1	
Recs50	5.8	EST (UniGene)	Hs.288309	1	
Recs51	6.0	Laminin B1 chain	M61916	1	RSS
Recs52	1.0	Matrix Gla protein (MGP)	M58549	1	
Recs53	2.5	Connective tissue growth factor	X78947	1	
Recs54	3.0	FLI-1/ERGB	Q50644	1	
Recs55	3.5	Thrombomodulin (TM)	M16552	1	RSS
Recs56	3.2	Transforming growth factor-β (TGF-β)	M60315	1	RSS
Recs57	3.1	HLA-E	X56841	3	
Recs58	3.0	Plasminogen activator inhibitor (PAI)	M16006	2	
Recs59	1.7	Keratin 18	M26326	2	
Recs60	1.8	IL-8	M26383	1	
Recs61	2.2	EST (UniGene)	Hs.105695	1	
Recs62	6.0	Thrombospondin	X14787	1	RSS
Recs63	1.7	Caveolin	Z18951	1	

[a] Numbers are assigned in order of appearance in Northern blot screening.
[b] FLC, full length cDNA clones were isolated for the functional validation of novel or functionally unanalyzed genes.
[c] RSS, clones that had previously been reported as responsive to shear stress (see text in detail).

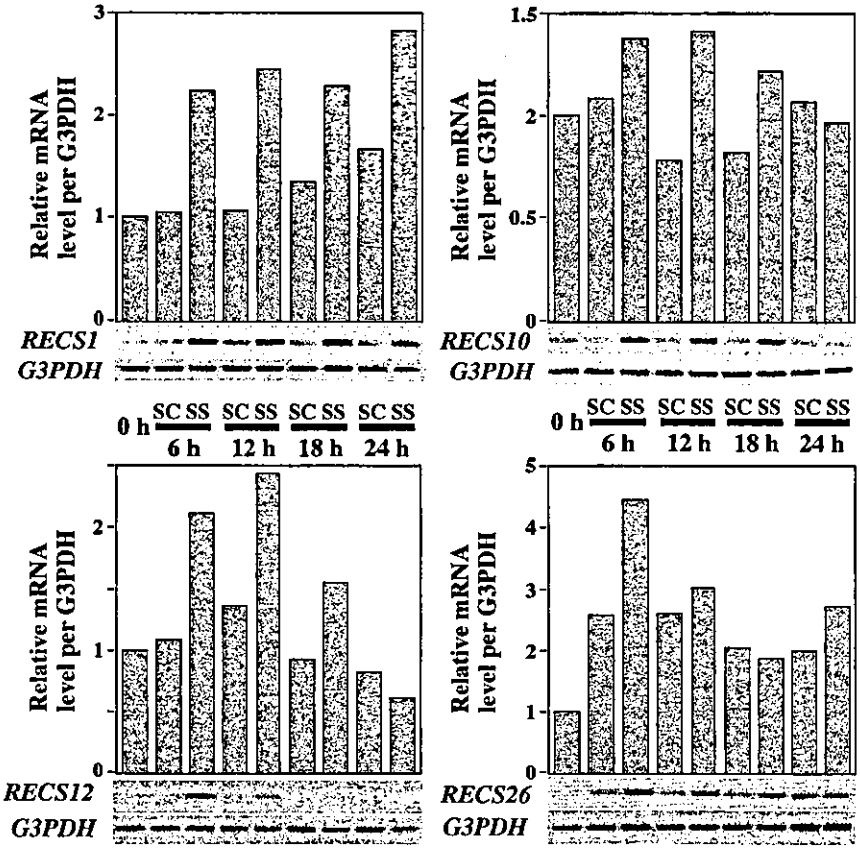

Fig. 4. Effect of steady laminar shear stress on the expression of *RECS* genes. After exposing HUVEC to steady laminar shear stress (18 dynes/cm^2; SS), total RNA was isolated at the indicated times, followed by semi-quantitative RT-PCR analysis. SC; static control. The number of PCR cycles was 23 for *RECS1*, 25 for *RECS10*, 28 for *RECS12*, 26 for *RECS26* and 20 for G3PDH. SYBR Green I staining of each gel is shown and bands were quantified with a FluorImager. The expression level of each *RECS* mRNA normalized to that of G3PDH was standardized to the value at 0 h, and is shown as the fold increase. For each gene, a representative result of at least three independent experiments is shown.

the S4R library, these novel or functionally unknown genes could also be relevant to atherosclerosis. Since most clones from the subtracted library contain partial cDNA inserts, we isolated full-length cDNAs for some *RECS* genes. Most of the genes whose full-length cDNAs were isolated, including *RECS1*, *RECS2* and *RECS24*, have recently been registered in the databases by other groups, although their functions are still unknown. *RECS1*, named as PP1201, shows significant homology to rat neural membrane protein 35 (NMP35) [24], whose predicted amino acid sequence is highly hydrophobic. *RECS2* appears to be a novel member of the immunoglobulin superfamily because it is weakly similar to Coxsackie and adenovirus receptor [25], and *RECS24* corresponds to a Unigene cluster, and is significantly homologous to known GTPase-activating proteins (GAP) such as rhoGAP [26]. However, the biological functions of these genes remain to be elucidated.

3.5. Some RECS genes are responsive to laminar shear stress

Since laminar rather than turbulent shear stress was utilized in most of the previous studies of this issue, we examined whether *RECS* genes are also upregulated by steady laminar shear stress in a parallel-plate flow chamber. We randomly selected five *RECS* genes of unknown function and whose responsiveness to laminar flow had not yet been demonstrated, and analyzed their mRNA levels in HUVEC by semiquantitative RT-PCR. The mRNA levels of four of the five genes, *RECS1*, *-10*, *-12* and *-26*, proved to be significantly elevated by laminar shear stress, compared with static controls at the same time points (Fig. 4). However, the remaining clone, *RECS7*, does not respond to laminar shear stress (data not shown). These results were expected, because the upregulation of representative laminar flow-responsive genes was confirmed by the data shown in Fig. 1,